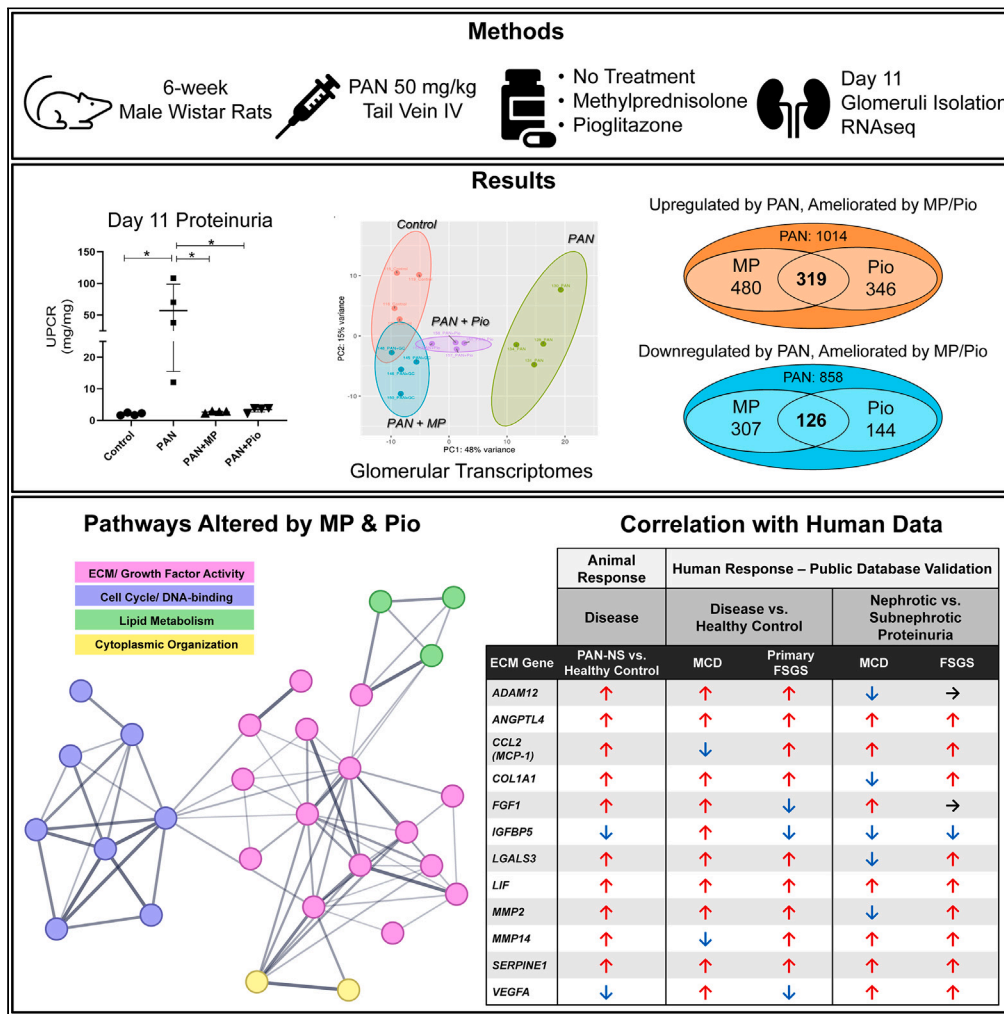


Article

# Glucocorticoid- and pioglitazone-induced proteinuria reduction in experimental NS both correlate with glomerular ECM modulation



Sagar Bhayana, Julie A. Dougherty, Yu Kamigaki, ..., Peter White, Bryce A. Kerlin, William E. Smoyer

william.smoyer@nationwidechildrens.org

**Highlights**

GC and Pio effectively ameliorated proteinuria in PAN-NS rats

RNAseq revealed 445 genes were similarly ameliorated with GC or Pio treatment of PAN-NS

ECM dysregulation was an early hallmark of PAN-NS, with amelioration by both treatments

Dysregulated genes in PAN-NS correlated with human data in patients with MCD and FSGS

Bhayana et al., iScience 27, 108631  
January 19, 2024 © 2023 The Authors.  
<https://doi.org/10.1016/j.isci.2023.108631>



## Article

## Glucocorticoid- and pioglitazone-induced proteinuria reduction in experimental NS both correlate with glomerular ECM modulation

Sagar Bhayana,<sup>1</sup> Julie A. Dougherty,<sup>1</sup> Yu Kamigaki,<sup>1</sup> Shipra Agrawal,<sup>1,2</sup> Saranga Wijeratne,<sup>3</sup> James Fitch,<sup>3</sup> Amanda P. Waller,<sup>1</sup> Katelyn J. Wolfgang,<sup>1</sup> Peter White,<sup>2,3</sup> Bryce A. Kerlin,<sup>1,2</sup> and William E. Smoyer<sup>1,2,4,\*</sup>

## SUMMARY

**Idiopathic nephrotic syndrome (NS) is a common glomerular disease. Although glucocorticoids (GC) are the primary treatment, the PPAR $\gamma$  agonist pioglitazone (Pio) also reduces proteinuria in patients with NS and directly protects podocytes from injury. Because both drugs reduce proteinuria, we hypothesized these effects result from overlapping transcriptional patterns. Systems biology approaches compared glomerular transcriptomes from rats with PAN-induced NS treated with GC vs. Pio and identified 29 commonly regulated genes-of-interest, primarily involved in extracellular matrix (ECM) remodeling. Correlation with clinical idiopathic NS patient datasets confirmed glomerular ECM dysregulation as a potential mechanism of injury. Cellular deconvolution *in silico* revealed GC- and Pio-induced amelioration of altered genes primarily within podocytes and mesangial cells. While validation studies are indicated, these analyses identified molecular pathways involved in the early stages of NS (prior to scarring), suggesting that targeting glomerular ECM dysregulation may enable a future non-immunosuppressive approach for proteinuria reduction in idiopathic NS.**

## INTRODUCTION

Idiopathic nephrotic syndrome (NS) is a common glomerular disease both in children and adults.<sup>1–6</sup> There are three major histologic variants of primary NS: minimal change disease (MCD), focal segmental glomerulosclerosis (FSGS), and membranous nephropathy (MN).<sup>7</sup> NS is a leading cause of chronic kidney disease in both children and adults, with more severe forms often progressing to end-stage kidney disease (ESKD).<sup>8</sup> The initial treatment for immune-mediated NS is high-dose daily glucocorticoids (GC), which are often associated with significant side effects.<sup>9,10</sup> While ~80% of children achieve clinical remission (i.e., resolution of proteinuria and edema) after 4–6 weeks of GC therapy, many children relapse, and as many as 50% of these children subsequently develop either frequent relapsing NS (FRNS) or steroid-dependent NS (SDNS). Such cases require recurrent and/or prolonged GC therapy or alternative immunosuppressive medications, which themselves are only effective in some patients and have significant toxicities. Moreover, ~20% of children and ~50% of adults present with or develop steroid-resistant NS (SRNS) and are at the highest risk for progression to ESKD.<sup>11,12</sup> For the aforementioned reasons, there is a critical need for the development of more effective and less toxic NS treatments.

An attractive alternative to new drug development is to repurpose existing Food and Drug Administration (FDA)-approved medications, which can markedly reduce costs and accelerate regulatory approval.<sup>13</sup> In this context, our group and others have reported that use of the PPAR $\gamma$  agonist pioglitazone (Pio) is associated with proteinuria reduction in adults and children with NS and that it may thus have potential as a non-immunosuppressive alternative or supplement to GC treatment for patients with NS.<sup>14–20</sup> Pio belongs to the thiazolidinedione (TZD) class of drugs and is FDA-approved for type 2 diabetes mellitus.<sup>21</sup> We previously reported significant proteinuria reduction after Pio treatment in the puromycin aminonucleoside (PAN)-induced rat model of NS (PAN-NS), which was comparable with the proteinuria reduction achieved by GC treatment.<sup>14,22</sup> Because both GC and Pio activate nuclear receptors (NR3C1 and PPAR $\gamma$ , respectively),<sup>14</sup> we hypothesized that the similar proteinuria-reducing effects of GC and Pio result from the induction of overlapping glomerular transcriptional patterns. To test this hypothesis, we compared the transcriptomes from glomeruli isolated from rats with PAN-NS in whom proteinuria was significantly reduced with either GC (immunosuppressive) or Pio (non-immunosuppressive) treatment. Our rationale was that the identification of overlapping glomerular transcriptional targets modulated by both GC and Pio would reveal common molecular pathways for proteinuria reduction in NS that could be exploited as potential future targets to treat NS.

<sup>1</sup>Center for Clinical and Translational Research, The Abigail Wexner Research Institute at Nationwide Children's Hospital, Columbus, OH 43205, USA

<sup>2</sup>Department of Pediatrics, The Ohio State University College of Medicine, Columbus, OH 43210, USA

<sup>3</sup>Institute for Genomic Medicine, The Abigail Wexner Research Institute at Nationwide Children's Hospital, Columbus, OH 43205, USA

<sup>4</sup>Lead contact

\*Correspondence: [william.smoyer@nationwidechildrens.org](mailto:william.smoyer@nationwidechildrens.org)

<https://doi.org/10.1016/j.isci.2023.108631>



## RESULTS

### Glucocorticoids and pioglitazone both partially restore nephrotic syndrome-associated glomerular gene expression dysregulation

We previously demonstrated that both methylprednisolone (MP, a representative GC) and Pio significantly reduced proteinuria in rats with PAN-induced NS.<sup>22</sup> To identify common molecular targets/pathways involved in proteinuria reduction, RNA sequencing (RNA-seq) was performed on glomeruli isolated from four rats from each of four experimental groups: (1) healthy controls, (2) PAN + sham treatment, (3) PAN + MP, and (4) PAN + Pio. As expected, PAN treatment induced significant proteinuria (urine protein to creatinine ratio [UPCR] =  $57.2 \pm 41.6$  mg/mg vs.  $2.03 \pm 0.42$  mg/mg in healthy controls; \* $p < 0.05$ ) at day 11 following a single PAN dose (Figure 1A). Significant proteinuria reduction was induced by treatment with either MP ( $2.64 \pm 0.32$  mg/mg [95% reduction]; \* $p < 0.05$ ) or Pio ( $3.45 \pm 0.82$  mg/mg [94% reduction]; \* $p < 0.05$ ). Subsequent unsupervised clustering performed on ~17,000 genes using principal-component analysis (PCA) revealed discrete transcriptional profiles for each treatment group (Figure 1B). The PAN-induced NS glomerular transcriptome was distinct and non-overlapping with the healthy control group. However, the glomerular transcriptomic profiles of the PAN + MP and PAN + Pio groups both revealed substantial transcriptomic shifts toward healthy controls. Notably, despite similar reductions in proteinuria, the MP and Pio transcriptomic profiles exhibited only modest overlap of their 95% confidence intervals (see colored ellipses), which suggested they have distinct transcriptional patterns contributing to proteinuria reduction (Figure 1B). Consistent with our hypothesis, we compared the transcriptomic profiles between MP and Pio to investigate potential common transcriptional targets for future NS therapeutics.

Next, we sequentially filtered the regulated genes based on strict selection criteria: (1) gene expression levels significantly different (false discovery rate [FDR]  $< 0.05$ ) between PAN vs. controls, (2) similar or comparable expression levels between PAN + MP and controls (FDR  $> 0.05$ ), (3) normalized read counts (NC)  $\geq 25$  in at least 3 samples in either group, and (4) genes that were well characterized and mappable to software platforms developed for Gene Ontology (GO) enrichment and pathway analysis. We identified 1,872 differentially expressed genes (DEGs), which were plotted as a heatmap (Figure 1C). A Venn diagram of these DEGs (Figure 2A) illustrates that PAN-NS glomeruli had 1,014 significantly upregulated and 858 significantly downregulated genes compared with healthy controls, identifying a distinct glomerular transcriptional dysregulation pattern associated with induction of PAN-NS. However, treatment with MP and Pio significantly reversed 480 (47%) and 346 (34%) of the upregulated genes (FDR  $< 0.05$ ), respectively. MP and Pio also significantly reversed 307 (36%) and 144 (17%) of the downregulated genes (FDR  $< 0.05$ ), respectively. Through overlap analysis, we identified 319 downregulated DEGs (i.e., genes significantly induced by PAN but reversed with treatments) and 126 upregulated DEGs (i.e., genes significantly suppressed by PAN but reversed by treatments) and categorized them as PAN-induced and PAN-suppressed DEGs, respectively (Figures 2A and 2B). This approach identified these two groups of DEGs as potential common molecular regulators of proteinuria, some of which could become future therapeutic targets for NS.

We then used the Database for Annotation, Visualization, and Integrated Discovery (DAVID) functional annotation cluster analysis tool,<sup>23</sup> an internet-based gene function annotation software application, to determine which pathways or biological processes were altered by these DEGs in glomeruli. DAVID analyses of the 319 PAN-induced genes with high enrichment scores ( $p < 0.05$ ) revealed that most of these DEGs were involved in cell cycle or mitosis, DNA binding, or DNA damage repair functions (Figures 2B and 2C). These findings suggested that PAN alters DNA homeostasis, which may impact the overall survival of glomerular cells. In addition, gene sets associated with ATP binding, microtubule activity, p53 signaling, protein kinase activity/phosphorylation, ubiquitination, transcription factor complexes, and extracellular matrix (ECM) organization were also significantly altered (Figures 2B and 2C). The precise molecular changes induced by PAN are not completely known, but these analyses suggested that glomerular DNA damage could be an initiating or early event resulting in PAN-induced proteinuria, partly in line with a published observation.<sup>24</sup>

An identical DAVID analysis of the 126 PAN-suppressed genes with high enrichment scores ( $p < 0.05$ ) revealed that most of these DEGs encompassed PDZ (first letters of the first three proteins discovered to share the domain postsynaptic density protein [PSD95], Drosophila disc large tumor suppressor [Dlg1], and zonula occludens-1 [ZO-1]) and sterile alpha motif (SAM) domains (Figures 2B and 2C). PDZ domains are involved in cell-cell contacts and anchoring membrane receptor proteins to cytoskeletal components.<sup>25,26</sup> Proteins containing SAM domains are involved in many different biological processes and bind to a variety of proteins and RNA.<sup>27,28</sup> In addition, gene sets associated with transcription factors, growth factors, and cytokines were also ameliorated by both MP and Pio treatments. Overall, the biological processes identified by these analyses highlighted a limited group of potentially important molecular pathways in glomeruli that are dysregulated during development of PAN-NS and ameliorated by treatments that effectively reduce proteinuria.

### Drug-nuclear receptor-DEG interaction network-based analysis of PAN-induced and PAN-suppressed DEGs identified 20 glomerular genes-of-interest (Method 1)

To attempt to identify drug targets using the PAN-induced and PAN-suppressed glomerular DEGs, we used the Ingenuity pathway analysis (IPA) software to screen for DEGs that were commonly regulated by both drugs (MP and Pio) and/or their canonical target nuclear receptors (NR3C1 and PPAR $\gamma$ , respectively). These analyses included the use of Ingenuity Knowledge Base (IKB), a repository of expertly curated biological interactions and functional annotations, to search among the selected DEGs for simultaneous interactions between the nuclear receptors (NR3C1 and PPAR $\gamma$ ) and their respective agonists (MP/dexamethasone and Pio, respectively). Although we used MP as the representative GC for our *in vivo* experiments, for these *in silico* analyses, we also included another GC and NR3C1 agonist, dexamethasone, to compensate for the paucity of available IKB repository data on MP. These analyses identified an interaction network formed among these drugs, their

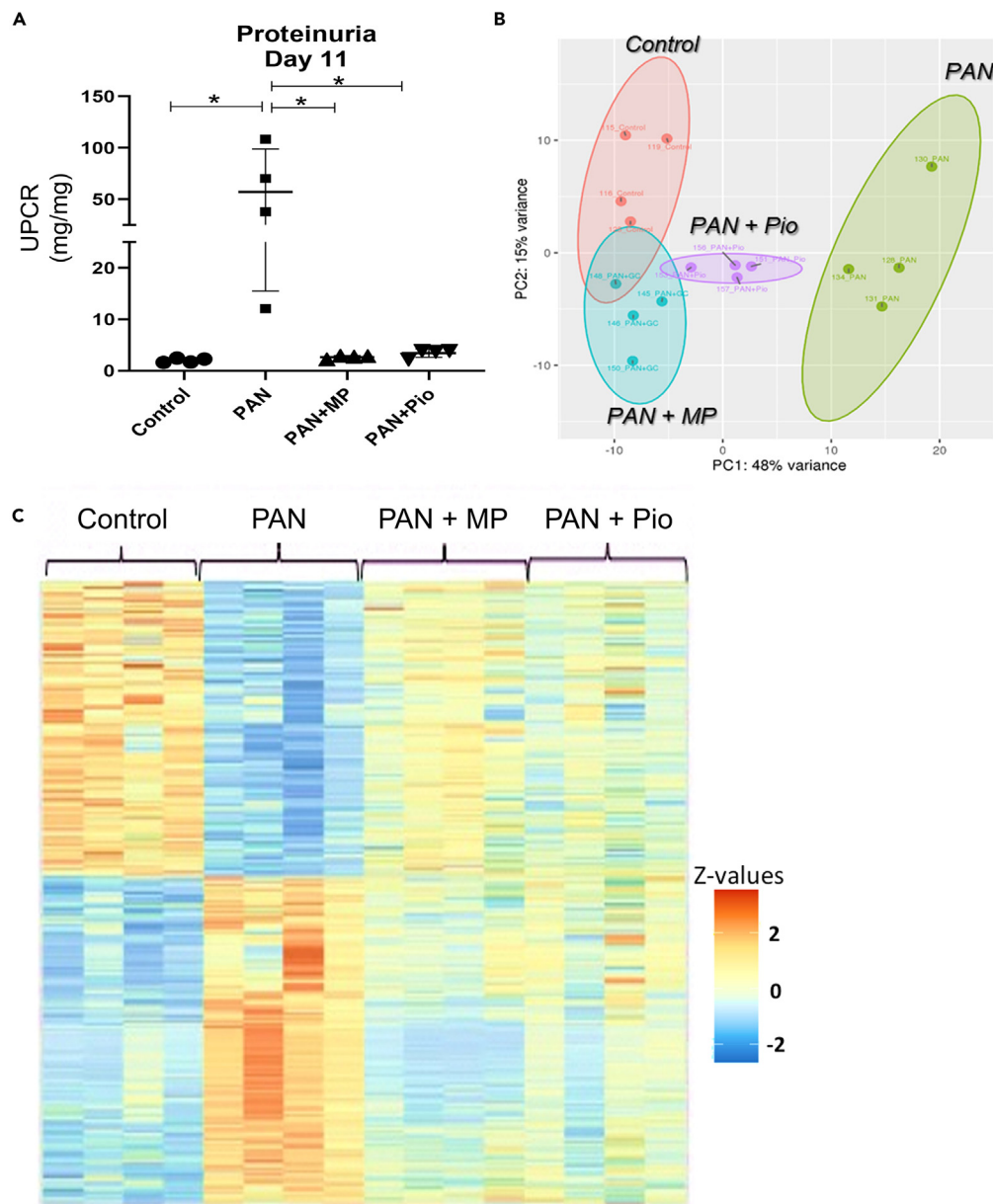


**Figure 1. Glucocorticoids and pioglitazone both ameliorate NS-associated glomerular gene expression profile dysregulation**

(A) UPCR of individual animals on Day 11 post-PAN, PAN + MP, PAN + Pio, or PBS control; n = 4 rats per group \*p < 0.05. Line with bars represents mean  $\pm$  SEM. (B) Principal-component analysis (PCA) plot representing unsupervised clustering of RNA-seq data. Colored bubbles (n = 4rats/group) represent the confidence interval of the combined four points, and each point within the bubble represents the transcriptome (~16,915 annotated genes) from each rat's pooled glomeruli. (C) Heatmap representation of 1,872 differentially expressed genes (DEGs). Red to blue scale denotes Z score.

nuclear receptors, and the glomerular DEGs, identifying 20 genes-of-interest (bolded and enlarged names in Figure 3A), whose protein products represented targets-of-interest. Because the proteins encoded by these genes are found in different cellular compartments (Table S1), we sought to identify any known interactions among them that might reveal critical molecular pathways relevant to proteinuria reduction. We used the *Search Tool for the Retrieval of Interacting Genes/Proteins* (STRING) database, a web resource of known and predicted protein-protein interactions.<sup>29</sup> Using k-means clustering, we identified four distinct clusters of protein-protein interactions encoded by these 20 genes-of-interest (dotted bubbles in Figure 3B), whereas the non-clustered/non-interactive nodes were removed from the interaction network. Consistent with the DAVID functional annotation analysis in Figure 2B, the STRING analysis predicted a limited group of specific protein interactions involved in glomerular cell function: (1) extracellular matrix homeostasis (extracellular matrix/growth factor activity), (2) DNA homeostasis (cell cycle and DNA binding), (3) lipid metabolism, and (4) cytoskeletal organization. These interaction analyses provided further support for

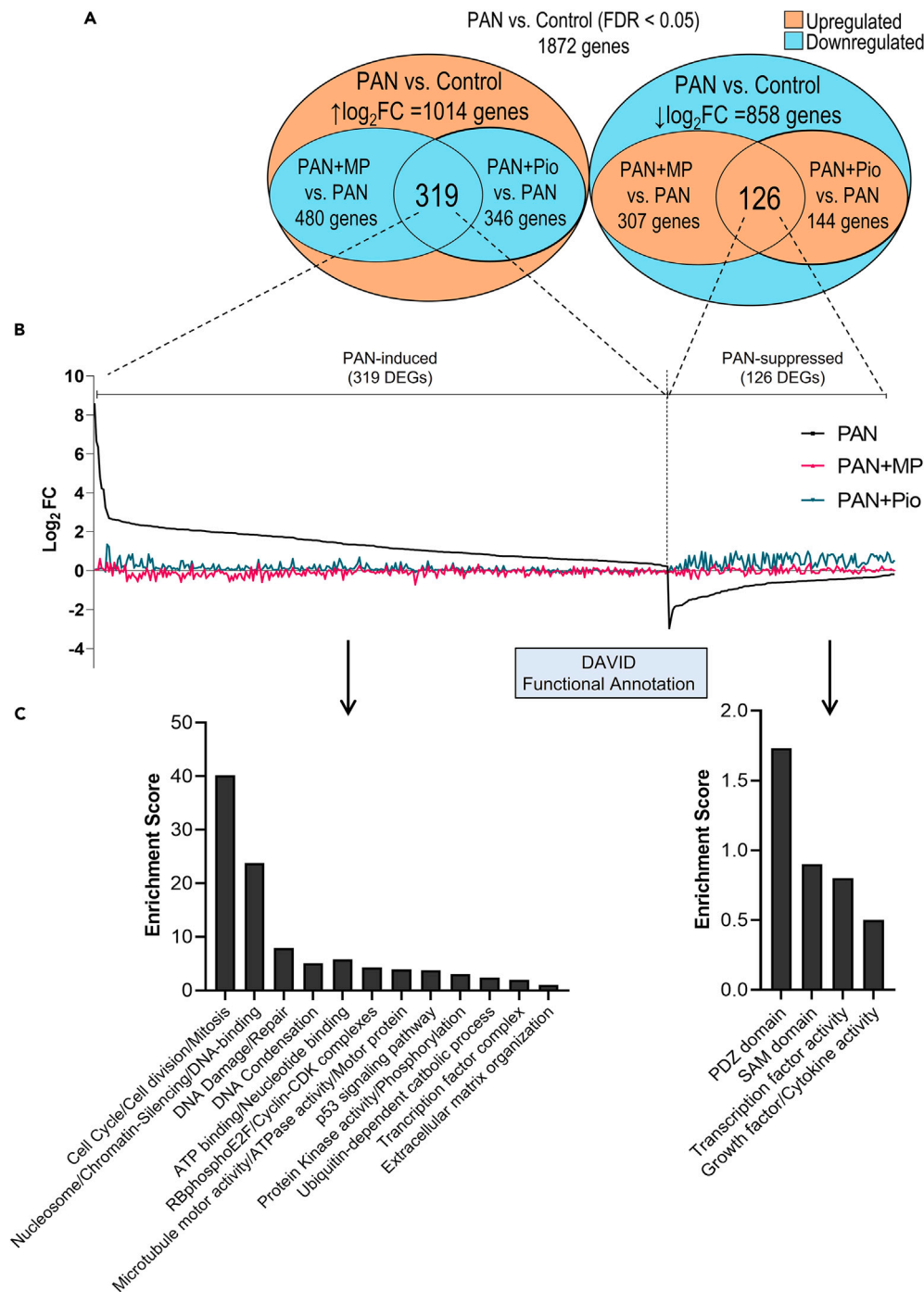


**Figure 2. Commonly regulated DEGs and pathways in GC and Pio-treated PAN-NS rats**

(A) Venn diagram representing the number of genes either upregulated or downregulated in PAN vs. Control (FDR < 0.05) and in treatment groups vs. PAN (FDR < 0.05). BLUE outer oval denotes downregulated genes, and ORANGE outer oval denotes upregulated genes. FDR is defined as false discovery rate, adjusted for multiple testing with the Benjamini-Hochberg procedure.

(B) Line plot representing the fold change ( $\log_2 FC$ ) of 319 and 126 DEGs significantly induced and suppressed by PAN, respectively (FDR < 0.05, PAN vs. Control), but significantly reversed by treatment groups (FDR < 0.05, PAN + MP, PAN + Pio vs. PAN). BLACK line denotes PAN. RED line denotes PAN + MP. GREEN line denotes PAN + Pio.

(C) Bar graph representing the functional annotation of 319 PAN-induced DEGs and 126 PAN-suppressed DEGs plotted based on enrichment scores using the Database for Annotation, Visualization, and Integrated Discovery (DAVID) functional annotation analysis platform. Enrichment score ranks the biological significance of gene groups based on the overall Fisher exact score of all enriched annotation terms.



**Figure 3. Continued**

(B) The corresponding protein-protein interactions of the 20 genes-of-interest determined by the STRING platform. Four clearly segregated clusters became apparent based on their respective biological annotation (biological processes, molecular function, cellular compartment). GRAY nodes represent proteins, and the line thickness between nodes signifies the strength of data supporting the association (i.e., thicker lines denote more available data sources showing the interaction, based on the STRING database). Interaction data sources included text mining, experiments, and databases. Minimum required interaction scores were set on medium confidence at 0.400. Clustering was performed using k-means clustering. Disconnected nodes were removed from the network.

dysregulation of a limited set of critical molecular pathways in glomeruli during PAN-NS and more importantly their restoration by treatment with two distinct classes of drugs that both effectively reduced proteinuria.

**Gene set enrichment analyses revealed restoration of dysregulated glomerular extracellular matrix genes as a common mechanism of proteinuria reduction (Method 2)**

Gene set enrichment analysis (GSEA) is commonly employed for pathway analysis and functional annotation of gene sets identified by RNA-seq using a molecular signature database that currently includes 22,596 gene sets.<sup>30</sup> We utilized GSEA as a second distinct method to identify glomerular genes that are dysregulated during PAN-NS and reversed in response to effective proteinuria reduction with both MP and Pio. We evaluated 17,000 genes using a global cutoff of  $\log_2(\text{Fold change}) \geq 2$  to enforce significant stringency in the identification of enriched gene sets. In comparison to healthy control rats, PAN significantly (FDR <0.05) induced dysregulation of glomerular gene sets associated with both extracellular matrix (*NABA\_MATRISOME ASSOCIATED*, *NABA\_ECM\_REGULATORS*, *NABA\_CORE\_MATRISOME*) and cyclins (*SA\_REG\_CASCADE\_OF\_CYCLIN\_EXPR*). On the other hand, treatments with either MP or Pio significantly (FDR <0.05) reversed PAN-induced dysregulation (heatmaps in Figure 4A). These findings further supported a mechanistic role for dysregulation of glomerular ECM proteins, as well as cyclins, in the pathogenesis of PAN-NS and that effective reduction of proteinuria (via two mechanistically distinct drug classes) was associated with reversal of this dysregulation.

As with the IPA analyses shown in Figure 3A, we used these GSEA-derived enriched gene sets to identify drug targets that were commonly regulated by both GC and Pio treatments (MP, dexamethasone, and Pio) and/or their nuclear receptors (NR3C1 and PPAR $\gamma$ , respectively). This interaction network identified 14 genes-of-interest likely to be involved in NR3C1 and PPAR $\gamma$  signaling processes (genes shown in bold in Figure 4B). We extended these findings to analyze protein-protein interactions among the proteins encoded by these 14 genes-of-interest using STRING analysis. Using k-means clustering, most of the targets clustered as an ECM-associated cluster, with matrix metalloproteinase 2 (*MMP2*) as a common interacting partner (Figure 4C).

Importantly, the genes-of-interest identified using the GSEA method (Method 2) overlapped significantly with the IPA analysis method (Method 1), and indeed most of the genes in common between these methods are involved in ECM remodeling (*ADAM12*, *MMP14*, *LGALS3*, *SERPINE1*). Collectively, these two distinct bioinformatic approaches identified 29 glomerular genes-of-interest likely to play mechanistic roles in both GC- and Pio-mediated proteinuria reduction in PAN-NS.

**Altered glomerular gene expression patterns in rats correlate extensively with those in patients with glomerular disease**

We sought to clinically validate the 29 genes-of-interest from the interaction networks based on Methods 1 and 2 (Figures 3B and 4C) to observe their changes in PAN-NS and possible amelioration with MP or Pio treatment (Figures 5, 6, and 7). We also compared the rat glomerular expression data with glomerular gene expression levels from the Nephroseq database for MCD, primary FSGS,<sup>31</sup> and diabetic kidney disease (DKD)<sup>32</sup> datasets.

*Extracellular matrix- and growth-factor-activity-related gene expression*

RNA-seq results revealed significant ( $p < 0.05$ ) up-regulation of *ADAM12*, *ANGPTL4*, *CCL2*, *COL1A1*, *LGALS3*, *LIF*, and *SERPINE1* and significant ( $p < 0.05$ ) down-regulation of *IGFBP5* and *VEGFA* in PAN-NS rats, compared with healthy rats (Figure 6A). Both MP and Pio treatment had a similar ameliorative effect on nearly all genes. However, PAN + MP and PAN + Pio differed significantly ( $p < 0.05$ ) in their expression of *ADAM12*, *CCL2*, and *COL1A1*, with MP having a more suppressive effect in each instance. MP treatment decreased *MMP2* expression to significantly ( $p < 0.05$ ) lower than that of healthy rats (Figure 6A).

To validate these findings in PAN-NS rats with patients with glomerular disease, we compared the expression patterns of these genes to those in kidney disease patients<sup>31</sup> using a publicly available, clinically derived glomerular gene expression datasets. First, we compared expression of the ECM-related genes-of-interest with that of patients with MCD ( $n = 7$ ) and primary FSGS ( $n = 8$ ) as compared with healthy controls ( $n = 9$ ) (NephroSeq: Hodgkin FSGS Glom).<sup>31</sup> Next, we further examined the same genes in a larger validation cohort recently published by Mariani et al. that compared MCD and FSGS patients with nephrotic vs. sub-nephrotic proteinuria (MCD:  $n = 42$  nephrotic,  $n = 24$  sub-nephrotic; FSGS:  $n = 44$  nephrotic,  $n = 42$  sub-nephrotic)<sup>33</sup> (Figures 6B and S1) (NephroSeq: Mariani Nephrotic Syndrome Glom). Overall, expression data from diseased glomeruli correlated extensively with that from PAN-NS rats, including 11 of 13 genes (85%) for primary FSGS and 8 of 13 genes (62%) for MCD as compared with healthy controls. FSGS patients with nephrotic proteinuria more closely correlated with PAN-NS rats as 11 of 13 genes (85%) trended similarly, compared with MCD patients with nephrotic proteinuria where 7 of 13 genes (54%) trended similarly. Despite their being distinctly different drug classes, both MP (immunosuppressive) and Pio (non-immunosuppressive) demonstrated similarly ameliorative effects on glomerular gene expression (Figure 6B) in association with their reduction in proteinuria in rats. MP and Pio showed similar trends in ameliorating dysregulated glomerular gene expression in patients with MCD (8 of 13, 62%) and



**Figure 4. GSEA enriched gene sets encoding genes involved in extracellular matrix remodeling and cell-cycle regulation (Method 2)**

Gene set enrichment analysis (GSEA) shows enrichment of (A) NABA\_MATRISOME\_ASSOCIATED, (B) NABA\_ECM\_REGULATORS, (C) NABA\_CORE\_MATRISOME, and (D) SA\_REG\_CASCADE\_OF\_CYCLIN\_EXPR related genes among the PAN, PAN + MP, and PAN + Pio genes that were ranked by normalized enrichment signal (NES) and q-value (FDR). The heatmap represents gene expression values of core-enriched genes, which account for the enrichment signal and thus represent the small subset of all the genes that participate in a biological process. Gene sets with a false discovery rate (FDR) value <0.05 after 1,000 permutations were considered significant.

primary FSGS (11 of 13, 85%). We also examined ECM gene expression in diabetic kidney disease (DKD) patients (n = 9) as compared with healthy transplant donors (n = 13) using the publicly available Woroniecka dataset (NephroSeq: Woroniecka Diabetes Glom).<sup>32</sup> DKD patient gene expression trended similar to PAN-NS rats for 8 of 13 genes (62%) (Figure S2), also demonstrating ECM dysregulation as a common defect in DKD, and notable similarity with our animal model of NS.

*Cytoplasmic-organization- and lipid-metabolism-related gene expression*

RNA-seq data demonstrated significantly (p < 0.05) increased expression of both ACTA2 and TAGLN in the diseased state (Figure 7A), which encode a cytoskeletal component and organizational regulator, respectively. Additionally, PAN-NS rats expressed significantly (p < 0.05) higher levels of lipid metabolism genes CPT1B and PDK4 and non-significantly increased LPL compared with healthy rats. Both MP and Pio treatment ameliorated expression of all 5 genes (100%), with CPT1B more significantly downregulated with MP treatment compared with Pio treatment (Figure 7B).

Comparing these findings to patients with glomerular disease, we found that both cytoplasmic organization genes were also upregulated in MCD and primary FSGS as compared with healthy patients and compared with those with sub-nephrotic proteinuria (Figures 7C and S2). Lipid metabolism genes had more heterogeneous expression in MCD and primary FSGS patients from either patient dataset as compared with PAN-NS rats (Figures 7C and S4). Again, MP and Pio both showed similar trends in ameliorating the glomerular expression of 3 of the 5 dysregulated cytoplasmic-organization- and lipid-metabolism-related genes (60%) in MCD and primary FSGS patients (Figure 7C). We also examined these genes' expression in diabetic kidney disease (DKD) patients as compared with healthy transplant donors.<sup>32</sup> DKD patient gene expression trended similar to PAN-NS rats for 4 of 5 genes (80%) (Figure S2), again showing a similar molecular signature for DKD to that of our animal model of NS.

*DNA-binding- and cell-cycle-related gene expression*

RNA-seq showed significantly (p < 0.05) increased glomerular expression of BIRC5, BRCA1, CDKN1A, CDKN2C, E2F1, and FOSB in diseased rats (Figure 8A). AIFM3, CDKN1B, and POU2F1 expression decreased with disease, but this change was not significant, whereas CDK4 expression remained similar to that in healthy animals (Figure 8A). MP and Pio treatment both demonstrated amelioration of 8 of the 9 dysregulated genes (89%), with MP showing significantly (p < 0.05) lower expression than Pio for BIRC5 and E2F1 (Figure 8A) in PAN-NS rats.

Comparing these findings with those from NS patients, we found that all groups of patients showed increased expression of BIRC5, CDKN1A, CDKN2C, and FOSB. However, expression of AIFM3, BRCA1, CDK4, CDKN1A, E2F1, and POU2F1 were affected differently in diseased patients (Figures 8B and S5). Similarly, we found that MP and Pio both showed comparable trends in ameliorating most of the dysregulated DNA-binding- and cell-cycle-related glomerular genes among patients with MCD (6 of 10, 60%) and primary FSGS (6 of 10, 60%) (Figure 8B). MCD and FSGS patients with nephrotic proteinuria had gene expression that trended very similarly to PAN-NS rats (Figure 8B). We also examined these genes' expression in DKD patients as compared with healthy transplant donorst.<sup>32</sup> DKD patient gene expression trended similar to PAN-NS rats for 6 of 10 genes (60%) (Figure S2), thus showing a similar molecular signature for DKD to that of our animal model of NS.

**Glucocorticoids and pioglitazone both reverse PAN-induced gene expression changes in podocyte- and mesangial-cell-specific, but not in endothelial-cell-specific, gene clusters**

Normal glomerular function depends on coordinated signaling between three resident glomerular cell lineages: podocytes, mesangial cells, and endothelial cells.<sup>34</sup> Although PAN-NS is a well-accepted model for the induction of glomerular proteinuria, its effects on gene expression in these three cell types *in vivo* have not been extensively studied. To analyze glomerular-cell-specific gene expression changes occurring during PAN-NS, we subdivided our glomerular transcriptomes into cell-specific subgroups using a published reference list of glomerular-cell-type-specific genes derived from healthy mouse glomeruli using single-cell RNA-seq to segregate podocyte-, endothelial-cell-, and mesangial-cell-specific genes.<sup>35</sup> For these analyses, we cross-tabulated our genes with the previously published mouse glomerular single-cell RNA-seq data using a cutoff of ≥ 500 normalized mRNA counts to select genes for this cell-type specificity analysis. After applying this criterion, we identified 66 podocyte-, 43 mesangial-, and 42 endothelial-cell-specific genes (Figures 9A–9C), including comparisons of mRNA changes among the Control vs. PAN, PAN + MP, and PAN + Pio treatment groups. Notably, the PAN-induced alterations were partially reversed following either MP or Pio treatment in both podocytes and mesangial cells, as exemplified by their respective PCA plots (see 95% confidence interval color shading) derived from these heatmaps (Figures 9D and 9E). In marked contrast to podocytes and mesangial cells, however, PAN treatment induced far fewer alterations in endothelial cells, and neither MP nor Pio treatment had notable effects on the transcriptional profiles of endothelial-cell-specific genes, despite their effectiveness in reducing proteinuria in the rats (Figure 9F).

In addition to these cell-specific findings, a combined PCA plot that integrated the aforementioned podocyte-, mesangial- and endothelial-specific genes also showed induction of significant dysregulation of glomerular gene expression by PAN, with partial reversal of these

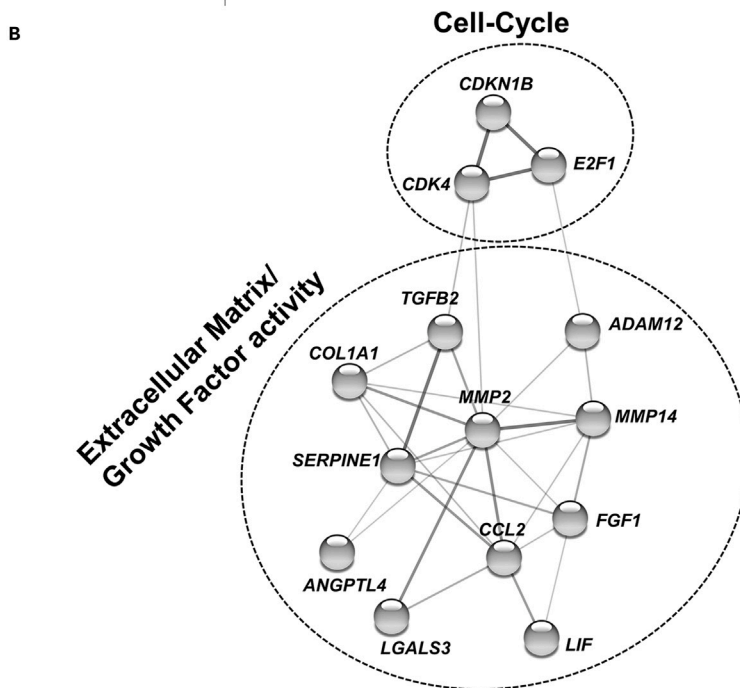
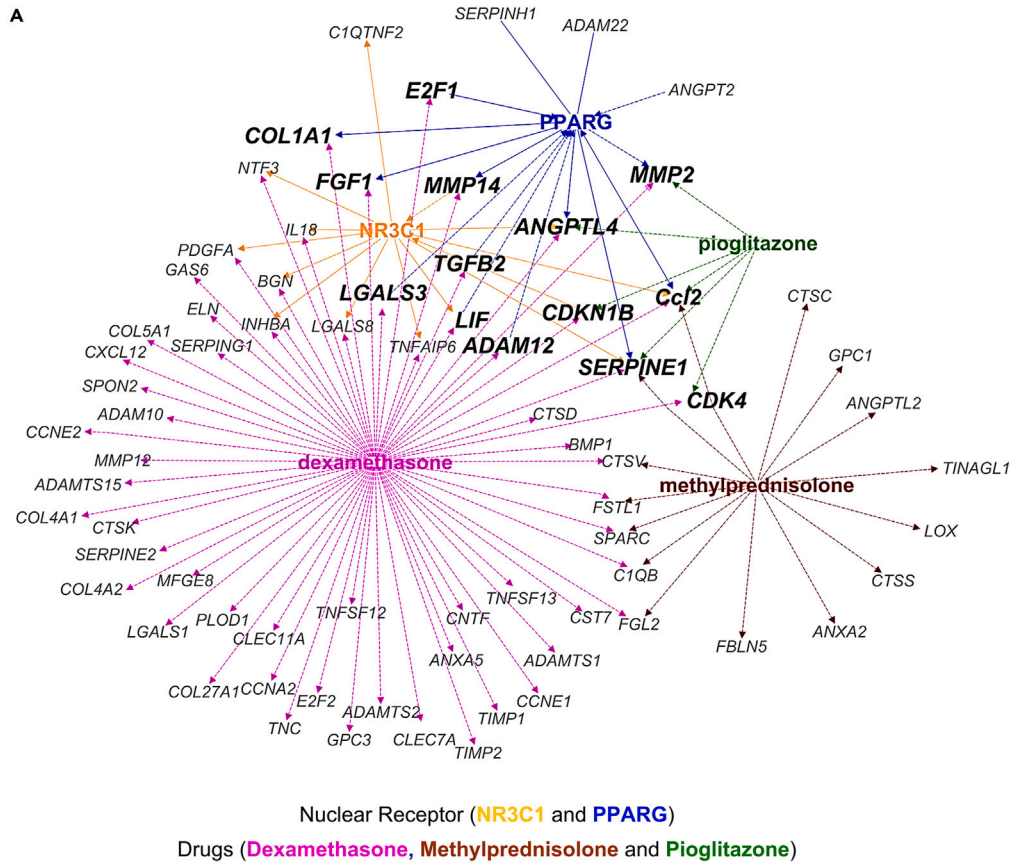


**Figure 5. Drug-nuclear receptor-DEG interaction network-based analysis of PAN-induced and PAN-suppressed DEGs revealed 20 genes-of-interest (Method 2)**

(A) Ingenuity pathway analysis (IPA)-based interaction network formed between nuclear receptor (NR3C1: YELLOW, PPARG: BLUE) and drug (dexamethasone: PINK, methylprednisolone: BROWN, pioglitazone: GREEN)—targets from the core-enriched genes from GSEA (shown in GRAY color). Genes in BOLD denote genes-of-interest that commonly interact with NR3C1 and PPARG receptors and/or their respective agonists.

(B) The corresponding protein-protein interactions of the 14 genes-of-interest determined by the STRING platform. Two clearly segregated clusters became apparent based on their respective biological annotation (biological processes, molecular function, cellular compartment). GRAY nodes represent proteins, and the line thickness between nodes signifies the strength of data supporting the association (i.e., thicker lines denote more available data sources showing the interaction, based on the STRING database). Interaction data sources included text mining, experiments, and databases. Minimum required interaction scores were set on medium confidence at 0.400. Clustering was performed using k-means clustering. Disconnected nodes were removed from the network.

changes following treatment with either MP or Pio (Figure S6). These findings suggested that the similar antiproteinuric effects of MP and Pio were likely mediated by common glomerular gene products or pathways, primarily via direct effects on podocytes and mesangial cells, or possibly via paracellular communication between podocytes and mesangial cells.

Focusing on the more impacted cell types, we analyzed the potential biological implications of the podocyte- and mesangial-cell-specific gene expression changes by incorporating these data into IPA-based function, disease, and toxicity analysis algorithms. Results indicated that, compared with PAN-NS, treatment with either MP or Pio led to similarly enhanced formation of filopodia and focal adhesions, enhanced microtubule dynamics and cytoskeleton reorganization, (Figure 9G) increased cell viability, decreased hyperplasia of mesangial cells, and decreased glomerular apoptosis (Figure 9H), all of which could serve to ameliorate injury to the glomerular filtration barrier.

## DISCUSSION

Nephrotic syndrome is characterized by dysregulation of the kidneys' glomerular filtering units leading to leakage of large amounts of plasma proteins into the urine. For NS, GCs, which are immunosuppressive, have remained the primary treatment for over 60 years despite myriad significant side effects. Pio, a non-immunosuppressive PPAR $\gamma$  agonist that is FDA-approved for type 2 diabetes mellitus, also reduced proteinuria in experimental NS in rats, reduced proteinuria in an adult patient with diabetes and FSGS,<sup>36</sup> reduced urinary podocyte loss in humans,<sup>37</sup> and protected podocytes from injury.<sup>22,37,38</sup> Moreover, a recent report revealed that Pio reduced proteinuria in children with complicated idiopathic NS in off-label use cases.<sup>10</sup> Together, these findings suggested that Pio could potentially be useful for proteinuria reduction in human NS. Because both GC and Pio activate nuclear receptors (NR3C1 and PPAR $\gamma$ , respectively),<sup>14</sup> we hypothesized that the similar proteinuria-reducing effects of GC and Pio likely result from overlapping glomerular transcriptional patterns. Therefore, we compared glomerular transcriptomes from rats with PAN-NS treated with either MP or Pio. Analyses included extensive *in silico* approaches, glomerular-cell-type-specific gene set deconvolution, and comparison of lead targets with published human MCD, primary FSGS, and DKD glomerular gene expression profiles. Collectively, these studies demonstrated that the similar antiproteinuric effects of MP and Pio in PAN-NS resulted largely from amelioration of dysregulated glomerular ECM-associated genes. Additionally, *in silico* glomerular cell deconvolution of these data using single-cell transcriptome profiles identified podocytes and mesangial cells as the cell types most altered by PAN treatment and ameliorated by treatment with MP and Pio.

Transcriptomic analyses revealed generally similar transcriptional regulation between the PAN + MP and PAN + Pio groups, with both treatment groups demonstrating amelioration of the PAN-induced changes associated with NS. Of note, many of the DEGs in the PAN + Pio group overlapped extensively with the PAN + MP group, suggesting that both drugs' proteinuria-reducing effects were likely due to alteration of similar molecular pathways within glomeruli. While it was expected that MP (a representative GC) treatment would ameliorate the expression of many glomerular genes dysregulated by PAN-induced NS, as prednisone is considered a front-line medication for NS,<sup>39</sup> it was of particular interest that Pio (a non-immunosuppressive drug) demonstrated a similar therapeutic pattern of reversibility of dysregulation. Interestingly, a total of 445 DEGs (319 PAN-induced + 126 PAN-suppressed) overlapped between MP and Pio treatment, suggesting that similar glomerular transcriptional responses underlie their antiproteinuric effects. Subsequent use of the DAVID functional annotation tool to investigate involved biological pathways revealed a modest list of potentially targetable biological pathways and processes associated with proteinuria reduction. While PAN treatment induced or suppressed several molecular pathways, one of the most significantly impacted was dysregulation of the glomerular ECM, which was identified by two distinct analytical methods in this study. Indeed, several of the genes-of-interest that overlapped between the two analytical methods were primarily involved with ECM (dys)regulation. These dysregulated genes also correlated extensively with the altered gene expression patterns in primary FSGS, MCD, and DKD patients published in the Nephroseq database, suggesting that ECM (dys)regulation in NS is clinically relevant and its therapeutic restoration may represent a future non-immunosuppressive approach for proteinuria reduction in NS.

Importantly, ECM remodeling has been recognized as a central feature of several progressive kidney diseases, including diabetic nephropathy, immunoglobulin A (IgA) nephropathy, and FSGS.<sup>40,41</sup> The current study identified amelioration of dysregulated glomerular ECM dynamics as a central molecular pathway common to both immunosuppressive- (i.e., MP) and non-immunosuppressive (i.e., Pio)-induced proteinuria reduction in NS. However, the specific molecular dysregulation between glomerular ECM production vs. degradation during glomerular disease progression remains poorly understood. In this context, the development of improved therapeutics to reduce and/or prevent disease progression will require a better understanding of glomerular ECM pathobiology, potentially including autocrine and/or paracrine ECM regulatory signaling among resident cells in the glomerulus.

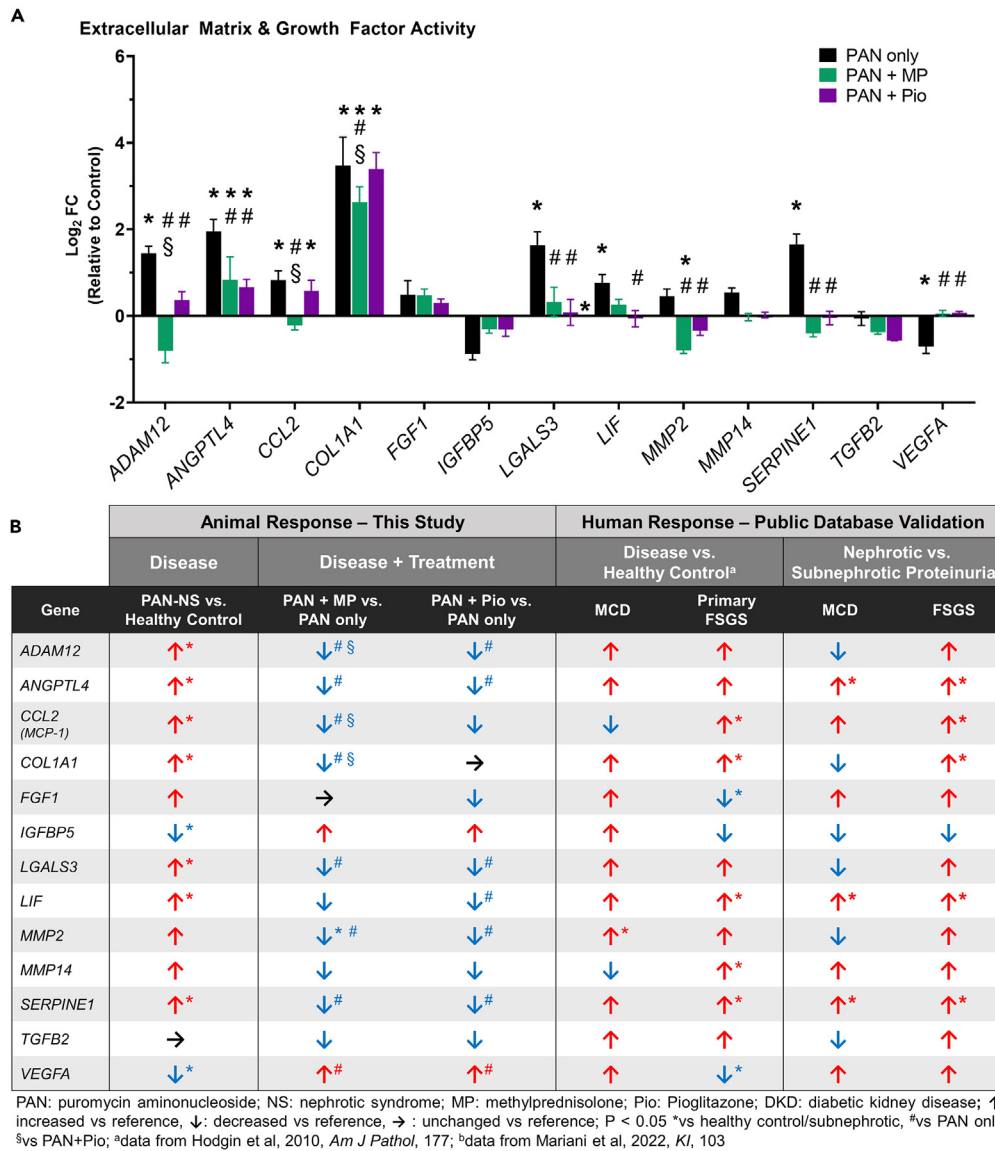


**Figure 6. Altered ECM- and growth-factor-activity-related glomerular gene expression patterns in rats correlate extensively with those in patients with glomerular disease**

(A) Rat glomerular RNAseq results of ECM-related genes with bar graphs mean ± SEM with \*p < 0.05 vs. Control; #p < 0.05 vs. PAN only, §p < 0.05 vs. PAN + Pio. (B) Hodgin MCD and FSGS glomerular data<sup>31</sup> and Woroniecka DKD (DN) glomerular data<sup>32</sup> from the Nephroseq database. Heatmap data are expressed as the log2-median centered intensity with fold changes relative to normal condition and significant changes noted as \*p < 0.05 vs. Normal Kidney/Healthy Donor. ANGPTL4 was not included in the DKD (DN) dataset.

Within glomeruli, multidirectional crosstalk occurs among resident podocytes, mesangial cells, and glomerular endothelial cells.<sup>34</sup> We thus leveraged the rat glomerular transcriptomics data to better understand the dynamics among these resident cells using published data from single-cell RNA-seq of each cell type in mouse glomeruli.<sup>35</sup> The glomerular gene dysregulation induced during PAN-NS and subsequent amelioration with MP or Pio treatment was seen primarily in podocytes and mesangial cells, with only modest changes observed in endothelial cells. Further, altered functions in podocytes and mesangial cells related to cytoskeletal maintenance, cellular viability, and kidney disease.

Regarding ECM dysregulation, our data correlate with other published studies in animals and humans. Our human glomerular analysis revealed increased LGALS3 expression in primary FSGS and DKD patients, which correlates with data from a glomerular ECM proteomics study of patients with collapsing FSGS also showing increased LGALS3 expression.<sup>42</sup> Sustained LGALS3 overexpression after tissue injury has been reported to lead to organ fibrosis<sup>43</sup> and elevated plasma protein levels of LGALS3 were associated with an increased risk of developing incident chronic kidney disease, especially in hypertensive patients.<sup>44</sup> LGALS3 also regulates cell adhesion and migration by regulating the expression of integrins α6β1 and α3β1, leading to actin cytoskeletal organization in glioma,<sup>45,46</sup> suggesting that its inhibition may be

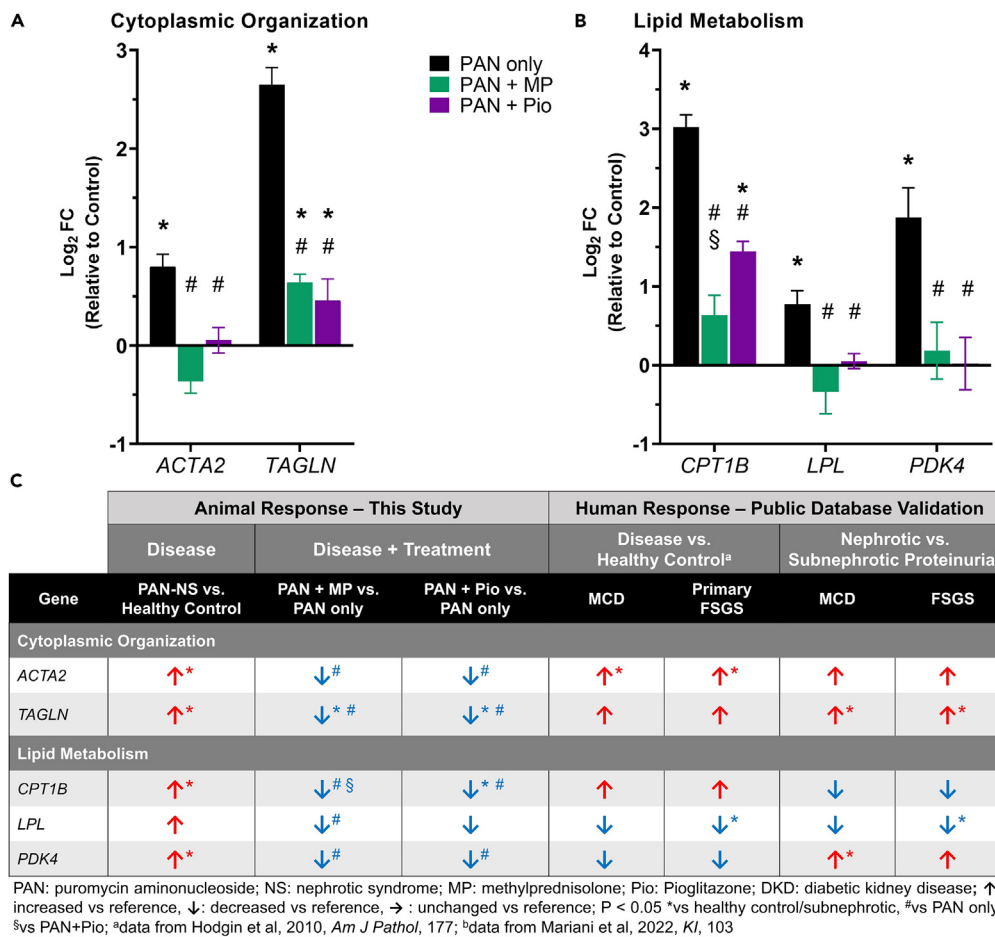


**Figure 7. Altered cytoplasmic-organization- and lipid metabolism-related glomerular gene expression patterns in rats correlate broadly with those in patients with glomerular disease**

Rat glomerular RNAseq results of (A) cytoplasmic-organization- and (B) lipid metabolism-related genes with bar graphs mean ± SEM with \*p < 0.05 vs. Control; #p < 0.05 vs. PAN only, §p < 0.05 vs. PAN + Pio. (C) Expression trends in PAN-NS rats, MCD and primary FSGS glomeruli,<sup>31</sup> DKD (DN) glomeruli,<sup>32</sup> and MP/Pio treated rats. \*p < 0.05 vs. Control/Normal Kidney/Healthy Donor; #p < 0.05 vs. PAN only, §p < 0.05 vs. PAN + Pio.

a biologically relevant treatment target in NS, given the importance of these integrins in podocyte adhesion to the glomerular basement membrane.<sup>47</sup>

This study also identified increased expression of *MMP2* in PAN-NS rats, and human primary FSGS, MCD, and DKD, and its amelioration with MP and Pio in PAN-NS rats. Matrix metalloproteinase 2, or *MMP2*, is a gelatinase capable of degrading glomerular basement membrane,<sup>48</sup> damaging the filtration barrier. *MMP2* is upregulated in response to stress, inflammation, or abnormal signaling and leads to fibrosis.<sup>49</sup> Our previous study analyzed plasma protein levels in NS patients and showed a significant decrease in *MMP2* after GC treatment in steroid-sensitive NS patients, which was absent in steroid-resistant patients.<sup>50</sup> Another study also observed increased plasma levels of *MMP2* in NS patients with active disease as compared with healthy controls and those in remission.<sup>51</sup>

Also of note was disease-induced expression of *SERPINE1*, which encodes plasminogen activator inhibitor type 1 (PAI-1) that along with plasminogen activator maintains the ECM and tissue homeostasis. Overexpression of PAI-1 inhibits plasmin functions and leads to fibrosis.<sup>52</sup> PAI-1 glomerular expression levels in renal biopsies showed significantly higher expression in MCD and FSGS kidneys compared with other glomerular diseases.<sup>53</sup>

Our data also align well with a recent report using kidney tissue transcriptomic data from patients with FSGS and MCD that identified TNF pathway activation as a risk factor for disease progression.<sup>33</sup> Notably, TNF pathway activation was characterized by a downstream increase in the urinary excretion of tissue inhibitor of metalloproteinase 1 (TIMP-1) and monocyte chemoattractant protein 1 (MCP-1),<sup>33</sup> which is the protein encoded by *CCL2*. We observed significantly increased *CCL2* in PAN-NS rats and humans with FSGS, lending further support to suggest *CCL2* as a candidate biomarker of primary FSGS.

Furthermore, we observed significantly increased glomerular expression of *ANGPTL4* in both PAN-NS rats and patients with primary FSGS and MCD. Studies have demonstrated increased expression of *ANGPTL4* in podocytes of rodent models and human MCD.<sup>54</sup> Interestingly,

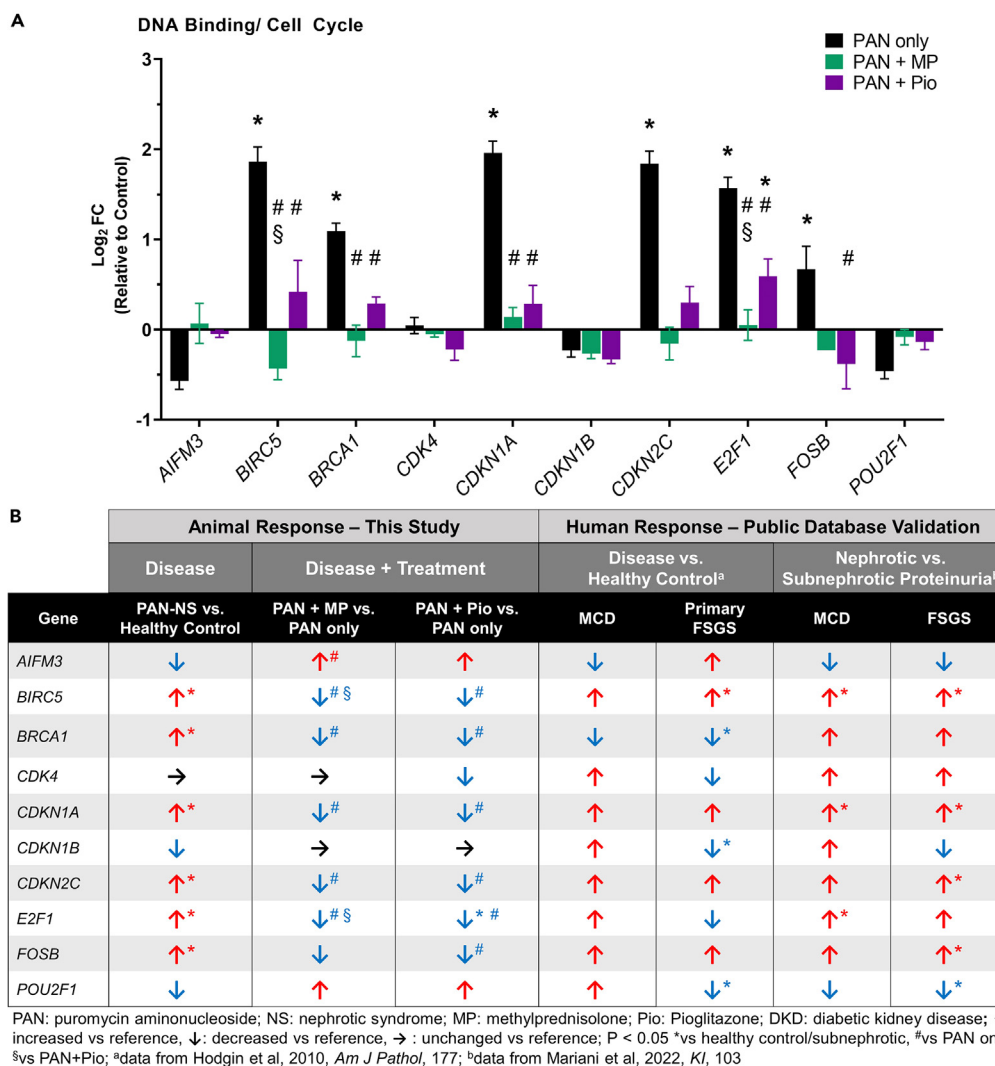


**Figure 8. Altered DNA binding- and cell-cycle-related glomerular gene expression patterns in rats moderately with those in patients with glomerular disease**

(A) Rat glomerular RNAseq results of DNA-binding- and cell-cycle-related genes with bar graphs mean ± SEM with \*p < 0.05 vs. Control; #p < 0.05 vs. PAN only, §p < 0.05 vs. PAN + Pio.

(B) Expression trends in PAN-NS rats, MCD glomeruli, primary FSGS glomeruli,<sup>31</sup> DKD (DN) glomeruli,<sup>32</sup> and MP/Pio treated rats. \*p < 0.05 vs. Control/Normal Kidney/Healthy Donor; #p < 0.05 vs. PAN only, §p < 0.05 vs. PAN + Pio. AIFM3 was not included in the DKD (DN) dataset.

podocyte-specific *ANGPTL4* overexpression caused massive proteinuria, whereas adipose-tissue-specific overexpression did not cause proteinuria.<sup>54</sup> *ANGPTL4* protein is secreted by podocytes into the circulation and has been suggested as a promising therapeutic target for NS.<sup>54</sup>

Of potential clinical relevance, the combined rat and human data demonstrate strong correlations between many of the glomerular genes dysregulated in rat PAN-NS and human patients with MCD and primary FSGS, with somewhat lesser correlations with DKD. In this context, it is notable that many of the dysregulated glomerular genes in rats had their expression ameliorated by treatment with GC and/or Pio. Although proteinuria reduction following treatment of FSGS patients with GC<sup>55–58</sup> and albuminuria and proteinuria reduction following treatment of DKD patients with Pio<sup>21,59</sup> are both well known, these findings provide a molecular rationale for the potential efficacy of Pio to reduce proteinuria in patients with FSGS. Indeed, the use of Pio as an adjunctive treatment for proteinuria reduction in children with NS and FSGS has recently been reported.<sup>20</sup>

In summary, these studies provide evidence that GC and Pio, although mechanistically distinct, both induced significant proteinuria reduction in PAN-NS at least in part via amelioration of dysregulated glomerular ECM genes. We also identified a highly refined list of glomerular candidate genes likely to play important roles in NS pathobiology, which may also be promising future molecular targets for non-immunosuppressive antiproteinuric therapy in NS. These genes were identified based on *in silico* comparisons of transcriptomic data derived from

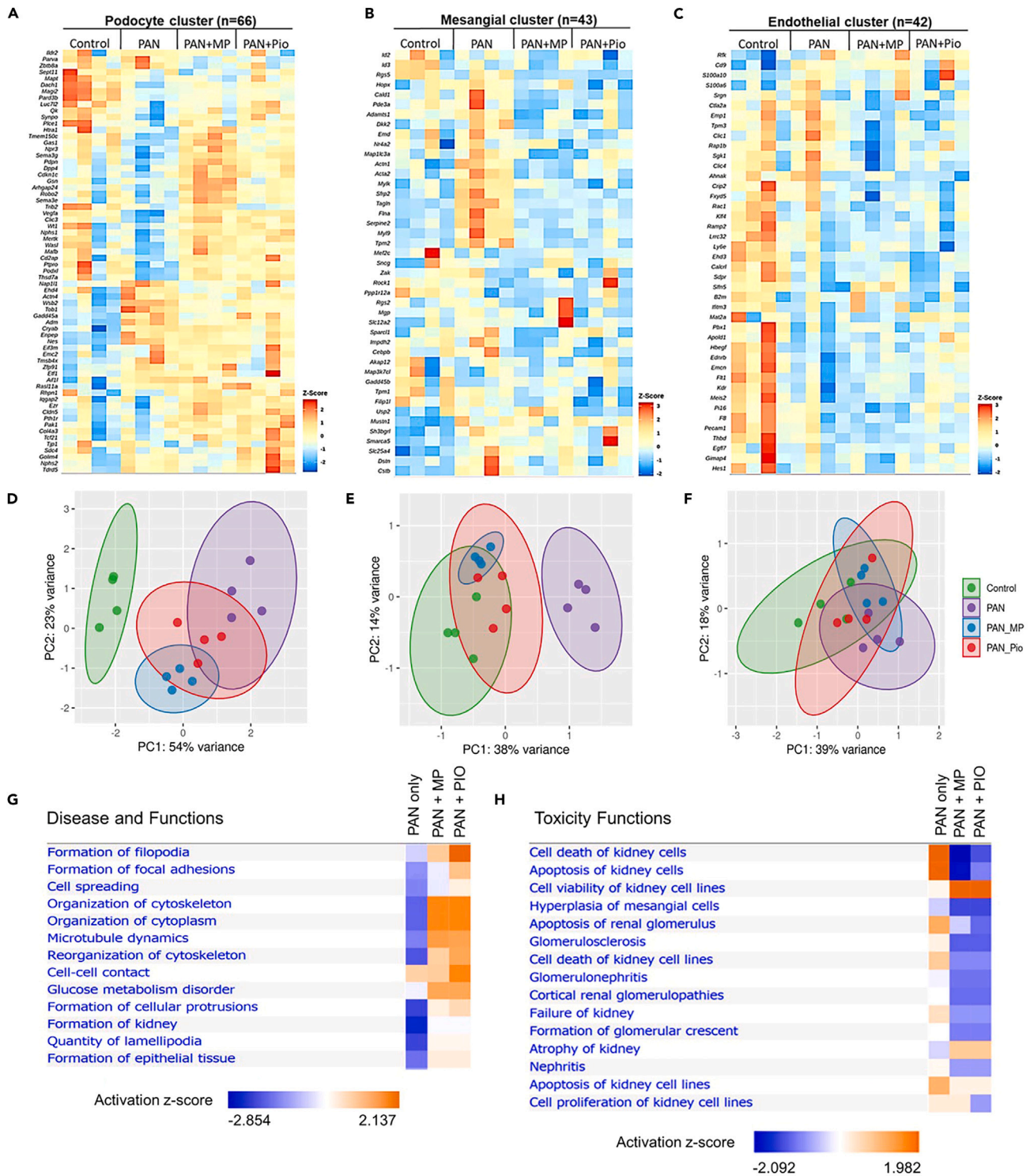


**Figure 9. Glucocorticoids and pioglitazone both reverse PAN-induced mRNA changes in podocyte- and mesangial-cell-specific, but not endothelial-cell-specific, gene clusters**

Heatmap representations (A–C) of treatment-induced gene expression changes in podocyte-specific genes [(A): podocyte cluster, n = 66 genes], mesangial-cell-specific genes [(B): mesangial cluster n = 43 genes], and endothelial-cell-specific genes [(C): endothelial cluster n = 42 genes]. The heatmap scale is based on raw Z scores calculated from the normalized read counts. The BLUE color denotes lower expression (i.e., downregulation), whereas the RED color denotes higher expression (i.e., upregulation). The normalized count cutoff for the selection of genes for each cluster was set as  $\geq 500$ .

**Figure 9. Continued**

(D) Podocyte-specific, (E) mesangial-cell-specific, and (F) endothelial-cell-specific PCA plots with ellipses as confidence intervals of four points per group combined, where each point of a sample group denotes 66 genes for podocyte cluster, 43 genes for mesangial cluster, and 42 genes for endothelial cluster. The heatmap compares the (G) gene function dynamics and (H) toxicities for PAN vs. PAN + MP vs. PAN + Pio treatments in respect to control, derived from IPA analyses of the combined podocyte + mesangial cell gene clusters. The color spectrum ranges from negative (inhibition) Z scores (shown in BLUE) to positive (activation) Z scores (shown in ORANGE).

both steroidal (i.e., immunosuppressive) and non-steroidal (i.e., non-immunosuppressive) treatments to reduce proteinuria in experimental NS. Additionally, our animal model data correlated well with dysregulation of glomerular gene expression seen in humans with FSGS, MCD, and DKD. Although validation studies are clearly indicated, these analyses identified molecular pathways involved in the early stages of NS (prior to scarring), suggesting that targeting glomerular ECM dysregulation may enable a future non-immunosuppressive approach for proteinuria reduction in NS.

**Limitations of the study**

Despite the integration of data from rats and human patients, this study has several limitations regarding the identification of targets-of-interest and possible mechanisms of action for Pio- and GC-induced proteinuria reduction in NS. For instance, although this study was discovery-based, subsequent validation of the role of specific genes in proteinuria reduction will require verification in other relevant NS models. Additionally, some genes-of-interest in the study had log<sub>2</sub> FC values < 2.0, and there were not significant differences between disease and treated animals (FDR > 0.05). Validation of these genes in a large cohort of patients or other animal models of NS could provide additional evidence for the importance of these pathways. Interestingly, increased expression of several targets correlated with increased protein expression in human studies, as discussed earlier. Moreover, validation at the protein level, perhaps with laser capture proteomics or spatial proteomics, would provide data on the functional importance of these targets. Also, while the current studies focused only on the overlapping molecules and pathways between GC- and Pio-induced proteinuria reduction, further investigation of the potential targets and pathways that were disparate between GC and Pio may also reveal additional potential targets for future NS therapy.

**STAR★METHODS**

Detailed methods are provided in the online version of this paper and include the following:

- KEY RESOURCES TABLE
- RESOURCE AVAILABILITY
  - Lead contact
  - Materials availability
  - Data and code availability
- EXPERIMENTAL MODEL AND STUDY PARTICIPANT DETAILS
- METHOD DETAILS
  - Proteinuria measurement
  - Glomerular isolation
  - Total RNA isolation and DNA digestion for RNA-Seq samples
  - RNA Library preparation and sequencing
  - RNA-seq data analysis
  - Functional gene annotation tools
  - Publicly available human dataset validation
  - In silico cellular deconvolution of rat glomerular RNAseq with mouse single cell RNAseq
- QUANTIFICATION AND STATISTICAL ANALYSIS

**SUPPLEMENTAL INFORMATION**

Supplemental information can be found online at <https://doi.org/10.1016/j.isci.2023.108631>.

**ACKNOWLEDGMENTS**

We thank Ms. Melinda Chanley for her technical assistance and Mrs. Emily Loughley for her assistance in manuscript preparation.

**Funding**

The present study was supported by a grant from the National Institutes of Health NIDDK R01 (DK 095059) to W.E.S..

**AUTHOR CONTRIBUTIONS**

Study design and conceptualization: S.B., S.A., W.E.S.

Methodology: S.B., S.A., S.W., J.F., A.P.W., K.W., B.A.K.

Investigation: S.B., J.A.D., Y.K., S.A., P.W., W.E.S.

Visualization: S.B., S.W., J.F., J.A.D., Y.K., W.E.S.

Funding acquisition: W.E.S.

Manuscript preparation and editing: S.B., J.A.D., Y.K., S.A., B.A.K., W.E.S.

## DECLARATION OF INTERESTS

Financial interests:

W.E.S. is a co-founder of NephKey Therapeutics, Inc.

S.B., S.A., and W.E.S. have filed patent # US 20230257817 A1.

Non-financial interests:

W.E.S. is on the Board of Directors of NephCure Kidney International and receives no compensation as a member of the Board of Directors.

## INCLUSION AND DIVERSITY

One or more of the authors of this paper self-identifies as an underrepresented ethnic minority in their field of research or within their geographical location.

One or more of the authors of this paper self-identifies as a gender minority in their field of research.

Received: April 10, 2023

Revised: October 31, 2023

Accepted: November 30, 2023

Published: December 2, 2023

## REFERENCES

- Trautmann, A., Boyer, O., Hodson, E., Bagga, A., Gipson, D.S., Samuel, S., Wetzels, J., Alhasan, K., Banerjee, S., Bhimma, R., et al. (2023). IPNA clinical practice recommendations for the diagnosis and management of children with steroid-sensitive nephrotic syndrome. *Pediatr. Nephrol.* **38**, 877–919.
- Chanchlani, R., and Parekh, R.S. (2016). Ethnic Differences in Childhood Nephrotic Syndrome. *Front. Pediatr.* **4**, 39.
- McGrogan, A., Franssen, C.F.M., and de Vries, C.S. (2011). The incidence of primary glomerulonephritis worldwide: a systematic review of the literature. *Nephrol. Dial. Transplant.* **26**, 414–430.
- Hu, R., Quan, S., Wang, Y., Zhou, Y., Zhang, Y., Liu, L., Zhou, X.J., and Xing, G. (2020). Spectrum of biopsy proven renal diseases in Central China: a 10-year retrospective study based on 34,630 cases. *Sci. Rep.* **10**, 10994.
- Mittal, P., Agarwal, S.K., Singh, G., Bhowmik, D., Mahajan, S., Dinda, A., and Bagchi, S. (2020). Spectrum of biopsy-proven renal disease in northern India: A single-centre study. *Nephrology* **25**, 55–62.
- O'Shaughnessy, M.M., Hogan, S.L., Poulton, C.J., Falk, R.J., Singh, H.K., Nickleleit, V., and Jennette, J.C. (2017). Temporal and Demographic Trends in Glomerular Disease Epidemiology in the Southeastern United States, 1986–2015. *Clin. J. Am. Soc. Nephrol.* **12**, 614–623.
- Eddy, A.A., and Symons, J.M. (2003). Nephrotic syndrome in childhood. *Lancet* **362**, 629–639.
- Kochanek, K.D., Murphy, S.L., Xu, J., and Arias, E. (2019). Deaths: Final Data for 2017. *Natl. Vital Stat. Rep.* **68**, 1–77.
- Valentini, R.P., and Smoyer, W.E. (2007). Nephrotic Syndrome. In *Clinical Pediatric Nephrology* K. H.W.S. Kher and S.P. Makker, eds. (Informa Healthcare), pp. 182–184.
- Greenbaum, L.A., Benndorf, R., and Smoyer, W.E. (2012). Childhood nephrotic syndrome—current and future therapies. *Nat. Rev. Nephrol.* **8**, 445–458.
- MacHardy, N., Miles, P.V., Massengill, S.F., Smoyer, W.E., Mahan, J.D., Greenbaum, L., Massie, S., Yao, L., Nagaraj, S., Lin, J.J., et al. (2009). Management patterns of childhood-onset nephrotic syndrome. *Pediatr. Nephrol.* **24**, 2193–2201.
- Ponticelli, C., Villa, M., Banfi, G., Cesana, B., Pozzi, C., Pani, A., Passerini, P., Farina, M., Grassi, C., and Baroli, A. (1999). Can prolonged treatment improve the prognosis in adults with focal segmental glomerulosclerosis? *Am. J. Kidney Dis.* **34**, 618–625.
- Pushpakom, S., Iorio, F., Eyers, P.A., Escott, K.J., Hopper, S., Wells, A., Doig, A., Williams, T., Latimer, J., McNamee, C., et al. (2019). Drug repurposing: progress, challenges and recommendations. *Nat. Rev. Drug Discov.* **18**, 41–58.
- Agrawal, S., Guess, A.J., Benndorf, R., and Smoyer, W.E. (2011). Comparison of direct action of thiazolidinediones and glucocorticoids on renal podocytes: protection from injury and molecular effects. *Mol. Pharmacol.* **80**, 389–399.
- Henique, C., Bollee, G., Lenoir, O., Dhaun, N., Camus, M., Chipont, A., Flosseau, K., Mandet, C., Yamamoto, M., Karras, A., et al. (2016). Nuclear Factor Erythroid 2-Related Factor 2 Drives Podocyte-Specific Expression of Peroxisome Proliferator-Activated Receptor gamma Essential for Resistance to Crescentic GN. *J. Am. Soc. Nephrol.* **27**, 172–188.
- Liu, H.F., Guo, L.Q., Huang, Y.Y., Chen, K., Tao, J.L., Li, S.M., and Chen, X.W. (2010). Thiazolidinedione attenuate proteinuria and glomerulosclerosis in Adriamycin-induced nephropathy rats via slit diaphragm protection. *Nephrology* **15**, 75–83.
- Yang, H.C., Ma, L.J., Ma, J., and Fogo, A.B. (2006). Peroxisome proliferator-activated receptor-gamma agonist is protective in podocyte injury-associated sclerosis. *Kidney Int.* **69**, 1756–1764.
- Zuo, Y., Yang, H.C., Potthoff, S.A., Najafian, B., Kon, V., Ma, L.J., and Fogo, A.B. (2012). Protective effects of PPARgamma agonist in acute nephrotic syndrome. *Nephrol. Dial. Transplant.* **27**, 174–181.
- Agrawal, S., He, J.C., and Tharoux, P.L. (2021). Nuclear receptors in podocyte biology and glomerular disease. *Nat. Rev. Nephrol.* **17**, 185–204.
- Hunley, T.E., Hidalgo, G., Ng, K.H., Shirai, Y., Miura, K., Beng, H.M., Wu, Q., Hattori, M., and Smoyer, W.E. (2023). Pioglitazone enhances proteinuria reduction in complicated pediatric nephrotic syndrome. *Pediatr. Nephrol.* **38**, 1127–1138.
- Sarafidis, P.A., Stafylas, P.C., Georgianos, P.I., Saratzis, A.N., and Lasaridis, A.N. (2010). Effect of thiazolidinediones on albuminuria and proteinuria in diabetes: a meta-analysis. *Am. J. Kidney Dis.* **55**, 835–847.
- Agrawal, S., Chanley, M.A., Westbrook, D., Nie, X., Kitao, T., Guess, A.J., Benndorf, R., Hidalgo, G., and Smoyer, W.E. (2016). Pioglitazone Enhances the Beneficial Effects of Glucocorticoids in Experimental Nephrotic Syndrome. *Sci. Rep.* **6**, 24392.
- Huang, D.W., Sherman, B.T., and Lempicki, R.A. (2009). Systematic and integrative analysis of large gene lists using DAVID bioinformatics resources. *Nat. Protoc.* **4**, 44–57.
- Marshall, C.B., Pippin, J.W., Krofft, R.D., and Shankland, S.J. (2006). Puromycin

- aminonucleoside induces oxidant-dependent DNA damage in podocytes in vitro and in vivo. *Kidney Int.* 70, 1962–1973.
25. Lee, H.-J., and Zheng, J.J. (2010). PDZ domains and their binding partners: structure, specificity, and modification. *Cell Commun. Signal.* 8, 8.
  26. Menon, R., Otto, E.A., Kokoruda, A., Zhou, J., Zhang, Z., Yoon, E., Chen, Y.C., Troyanskaya, O., Spence, J.R., Kretzler, M., and Cebrian, C. (2018). Single-cell Analysis of Progenitor Cell Dynamics and Lineage Specification in the Human Fetal Kidney. *Development* 145.
  27. Aviv, T., Lin, Z., Lau, S., Rendl, L.M., Sicheri, F., and Smibert, C.A. (2003). The RNA-binding SAM domain of Smaug defines a new family of post-transcriptional regulators. *Nat. Struct. Biol.* 10, 614–621.
  28. Green, J.B., Gardner, C.D., Wharton, R.P., and Aggarwal, A.K. (2003). RNA recognition via the SAM domain of Smaug. *Mol. Cell* 11, 1537–1548.
  29. Szklarczyk, D., Gable, A.L., Lyon, D., Junge, A., Wyder, S., Huerta-Cepas, J., Simonovic, M., Doncheva, N.T., Morris, J.H., Bork, P., et al. (2019). STRING v11: protein-protein association networks with increased coverage, supporting functional discovery in genome-wide experimental datasets. *Nucleic Acids Res.* 47, D607–D613.
  30. Subramanian, A., Tamayo, P., Mootha, V.K., Mukherjee, S., Ebert, B.L., Gillette, M.A., Paulovich, A., Pomeroy, S.L., Golub, T.R., Lander, E.S., and Mesirov, J.P. (2005). Gene set enrichment analysis: a knowledge-based approach for interpreting genome-wide expression profiles. *Proc. Natl. Acad. Sci. USA* 102, 15545–15550.
  31. Hodgin, J.B., Borczuk, A.C., Nasr, S.H., Markowitz, G.S., Nair, V., Martini, S., Eichinger, F., Vining, C., Berthier, C.C., Kretzler, M., and D'Agati, V.D. (2010). A molecular profile of focal segmental glomerulosclerosis from formalin-fixed, paraffin-embedded tissue. *Am. J. Pathol.* 177, 1674–1686.
  32. Woroniecka, K.I., Park, A.S.D., Mohtai, D., Thomas, D.B., Pullman, J.M., and Susztak, K. (2011). Transcriptome analysis of human diabetic kidney disease. *Diabetes* 60, 2354–2369.
  33. Mariani, L.H., Eddy, S., AlAkwa, F.M., McCown, P.J., Harder, J.L., Nair, V., Eichinger, F., Martini, S., Ademola, A.D., Boima, V., et al. (2023). Precision nephrology identified tumor necrosis factor activation variability in minimal change disease and focal segmental glomerulosclerosis. *Kidney Int.* 103, 565–579.
  34. Kitching, A.R., and Hutton, H.L. (2016). The Players: Cells Involved in Glomerular Disease. *Clin. J. Am. Soc. Nephrol.* 11, 1664–1674.
  35. Karaiskos, N., Rahmatollahi, M., Boltengagen, A., Liu, H., Hoehne, M., Rinschen, M., Schermer, B., Benzing, T., Rajewsky, N., Kocks, C., et al. (2018). A Single-Cell Transcriptome Atlas of the Mouse Glomerulus. *J. Am. Soc. Nephrol.* 29, 2060–2068.
  36. Sharma, A., Bourey, R.E., Edwards, J.C., Brink, D.S., and Albert, S.G. (2021). Nephrotic range proteinuria associated with focal segmental glomerulosclerosis reversed with pioglitazone therapy in a patient with Dunnigan type lipodystrophy. *Diabetes Res. Clin. Pract.* 172, 108620.
  37. Nakamura, T., Ushiyama, C., Osada, S., Hara, M., Shimada, N., and Koide, H. (2001). Pioglitazone reduces urinary podocyte excretion in type 2 diabetes patients with microalbuminuria. *Metabolism* 50, 1193–1196.
  38. Xing, Y., Ye, S., Hu, Y., and Chen, Y. (2012). Podocyte as a potential target of inflammation: role of pioglitazone hydrochloride in patients with type 2 diabetes. *Endocr. Pract.* 18, 493–498.
  39. Ponticelli, C., and Passerini, P. (1994). Treatment of the nephrotic syndrome associated with primary glomerulonephritis. *Kidney Int.* 46, 595–604.
  40. Clotet-Freixas, S., and Konvalinka, A. (2021). Too Little or Too Much? Extracellular Matrix Remodeling in Kidney Health and Disease. *J. Am. Soc. Nephrol.* 32, 1541–1543.
  41. Oomura, A., Nakamura, T., Arakawa, M., Oshima, A., and Isemura, M. (1989). Alterations in the extracellular matrix components in human glomerular diseases. *Virchows Arch. A Pathol. Anat. Histopathol.* 415, 151–159.
  42. Merchant, M.L., Barati, M.T., Caster, D.J., Hata, J.L., Hobeika, L., Coventry, S., Brier, M.E., Wilkey, D.W., Li, M., Rood, I.M., et al. (2020). Proteomic Analysis Identifies Distinct Glomerular Extracellular Matrix in Collapsing Focal Segmental Glomerulosclerosis. *J. Am. Soc. Nephrol.* 31, 1883–1904.
  43. Suthahar, N., Meijers, W.C., Silljé, H.H.W., Ho, J.E., Liu, F.T., and de Boer, R.A. (2018). Galectin-3 Activation and Inhibition in Heart Failure and Cardiovascular Disease: An Update. *Theranostics* 8, 593–609.
  44. Rebholz, C.M., Selvin, E., Liang, M., Ballantyne, C.M., Hoogeveen, R.C., Aguilar, D., McEvoy, J.W., Grams, M.E., and Coresh, J. (2018). Plasma galectin-3 levels are associated with the risk of incident chronic kidney disease. *Kidney Int.* 93, 252–259.
  45. Le Mercier, M., Fortin, S., Mathieu, V., Kiss, R., and Lefranc, F. (2010). Galectins and gliomas. *Brain Pathol.* 20, 17–27.
  46. Debray, C., Vereecken, P., Belot, N., Teillard, P., Brion, J.P., Pandolfo, M., and Pochet, R. (2004). Multifaceted role of galectin-3 on human glioblastoma cell motility. *Biochem. Biophys. Res. Commun.* 325, 1393–1398.
  47. Pozzi, A., Jarad, G., Moeckel, G.W., Coffa, S., Zhang, X., Gewin, L., Eremina, V., Hudson, B.G., Borza, D.B., Harris, R.C., et al. (2008). Beta1 integrin expression by podocytes is required to maintain glomerular structural integrity. *Dev. Biol.* 316, 288–301.
  48. Martin, J., Eynstone, L., Davies, M., and Steadman, R. (2001). Induction of metalloproteinases by glomerular mesangial cells stimulated by proteins of the extracellular matrix. *J. Am. Soc. Nephrol.* 12, 88–96.
  49. Cheng, Z., Limbu, M.H., Wang, Z., Liu, J., Liu, L., Zhang, X., Chen, P., and Liu, B. (2017). MMP-2 and 9 in Chronic Kidney Disease. *Int. J. Mol. Sci.* 18, 776.
  50. Agrawal, S., Merchant, M.L., Kino, J., Li, M., Wilkey, D.W., Gaweda, A.E., Brier, M.E., Chanley, M.A., Gooding, J.R., Sumner, S.J., et al. (2020). Predicting and Defining Steroid Resistance in Pediatric Nephrotic Syndrome Using Plasma Proteomics. *Kidney Int. Rep.* 5, 66–80.
  51. Bauer, C., Piani, F., Banks, M., Ordoñez, F.A., de Lucas-Collantes, C., Oshima, K., Schmidt, E.P., Zakharevich, I., Segarra, A., Martinez, C., et al. (2022). Minimal Change Disease Is Associated With Endothelial Glycocalyx Degradation and Endothelial Activation. *Kidney Int. Rep.* 7, 797–809.
  52. Flevaris, P., and Vaughan, D. (2017). The Role of Plasminogen Activator Inhibitor Type-1 in Fibrosis. *Semin. Thromb. Hemost.* 43, 169–177.
  53. Hamano, K., Iwano, M., Akai, Y., Sato, H., Kubo, A., Nishitani, Y., Uyama, H., Yoshida, Y., Miyazaki, M., Shiki, H., et al. (2002). Expression of glomerular plasminogen activator inhibitor type 1 in glomerulonephritis. *Am. J. Kidney Dis.* 39, 695–705.
  54. Clement, L.C., Avila-Casado, C., Macé, C., Soria, E., Bakker, W.W., Kersten, S., and Chugh, S.S. (2011). Podocyte-secreted angiopoietin-like-4 mediates proteinuria in glucocorticoid-sensitive nephrotic syndrome. *Nat. Med.* 17, 117–122.
  55. Kidney Disease Improving Global Outcomes KDIGO Glomerular Diseases Work Group, Adler, S.G., Barratt, J., Bridoux, F., Burdige, K.A., Chan, T.M., Cook, H.T., Fervenza, F.C., Gibson, K.L., Glassock, R.J., et al. (2021). KDIGO 2021 Clinical Practice Guideline for the Management of Glomerular Diseases. *Kidney Int.* 100, S1–S276.
  56. Korbet, S.M., Schwartz, M.M., and Lewis, E.J. (1994). Primary focal segmental glomerulosclerosis: clinical course and response to therapy. *Am. J. Kidney Dis.* 23, 773–783.
  57. Goumenos, D.S., Tsagalas, G., El Nahas, A.M., Shortland, J.R., Davlouros, P., Vlachojannis, J.G., and Brown, C.B. (2006). Immunosuppressive Treatment of Idiopathic Focal Segmental Glomerulosclerosis: A Five-Year Follow-Up Study. *Nephron Clin. Pract.* 104, c75–c82.
  58. Huang, J., Lin, L., Xie, J., Li, X., Shen, P., Pan, X., Ren, H., and Chen, N. (2018). Glucocorticoids in the treatment of patients with primary focal segmental glomerulosclerosis and moderate proteinuria. *Clin. Exp. Nephrol.* 22, 1315–1323.
  59. Zhou, Y., Huang, Y., Ji, X., Wang, X., Shen, L., and Wang, Y. (2020). Pioglitazone for the Primary and Secondary Prevention of Cardiovascular and Renal Outcomes in Patients with or at High Risk of Type 2 Diabetes Mellitus: A Meta-Analysis. *J. Clin. Endocrinol. Metab.* 105, dgz252–1681.
  60. Agrawal, S., Guess, A.J., Chanley, M.A., and Smoyer, W.E. (2014). Albumin-induced podocyte injury and protection are associated with regulation of COX-2. *Kidney Int.* 86, 1150–1160.
  61. Smoyer, W.E., Gupta, A., Mundel, P., Ballew, J.D., and Welsh, M.J. (1996). Altered expression of glomerular heat shock protein 27 in experimental nephrotic syndrome. *J. Clin. Invest.* 97, 2697–2704.
  62. Barisoni, L., Nast, C.C., Jennette, J.C., Hodgin, J.B., Herzenberg, A.M., Lemley, K.V., Conway, C.M., Kopp, J.B., Kretzler, M., Lienczewski, C., et al. (2013). Digital pathology evaluation in the multicenter Nephrotic Syndrome Study Network (NEPTUNE). *Clin. J. Am. Soc. Nephrol.* 8, 1449–1459.

63. Osafo, C., Raji, Y.R., Burke, D., Tayo, B.O., Tiffin, N., Moxey-Mims, M.M., Rasooly, R.S., Kimmel, P.L., Ojo, A., Adu, D., et al. (2015). Human Heredity and Health (H3) in Africa Kidney Disease Research Network: A Focus on Methods in Sub-Saharan Africa. *Clin. J. Am. Soc. Nephrol.* *10*, 2279–2287.
64. Yasuda, Y., Cohen, C.D., Henger, A., and Kretzler, M.; European Renal cDNA Bank ERCB Consortium (2006). Gene expression profiling analysis in nephrology: towards molecular definition of renal disease. *Clin. Exp. Nephrol.* *10*, 91–98.
65. Schmid, H., Boucherot, A., Yasuda, Y., Henger, A., Brunner, B., Eichinger, F., Nitsche, A., Kiss, E., Bleich, M., Gröne, H.J., et al. (2006). Modular activation of nuclear factor-kappaB transcriptional programs in human diabetic nephropathy. *Diabetes* *55*, 2993–3003.
66. Gadegbeku, C.A., Gipson, D.S., Holzman, L.B., Ojo, A.O., Song, P.X.K., Barisoni, L., Sampson, M.G., Kopp, J.B., Lemley, K.V., Nelson, P.J., et al. (2013). Design of the Nephrotic Syndrome Study Network (NEPTUNE) to evaluate primary glomerular nephropathy by a multidisciplinary approach. *Kidney Int.* *83*, 749–756.

## STAR★METHODS

### KEY RESOURCES TABLE

REAGENT or RESOURCE	SOURCE	IDENTIFIER
<b>Chemicals, peptides, and recombinant proteins</b>		
Puromycin aminonucleoside (PAN)	Millipore Sigma	P7310; 58-60-6
Methylprednisolone (Solumedrol)		
Pioglitazone	Enzo Life Sciences	ALX-270-367-M005; 111025-46-8
$\beta$ -mercaptoethanol	Millipore Sigma	M6250; 60-24-2
DNase I	Ambion	AM2222;
<b>Deposited data</b>		
RNAseq normalized data from this study	Gene Expression Omnibus (GEO)	GEO: GSE2480
<b>Experimental models: Organisms/strains</b>		
Wistar outbred rats, male, 125-149g, approx. 5 weeks	Envigo	Hsd:WI, RRID: RGD_737960
<b>Software and algorithms</b>		
Cutadapt	<a href="https://cutadapt.readthedocs.io/en/stable/index.html">https://cutadapt.readthedocs.io/en/stable/index.html</a>	v1.10
STAR (RNAseq aligner)	NCBI; <a href="http://bioinformatics.oxfordjournals.org/content/29/1/15">http://bioinformatics.oxfordjournals.org/content/29/1/15</a>	v2.5.0c
HTSeq (Python)	<a href="http://www-huber.embl.de/users/anders/HTSeq/doc/count.html">http://www-huber.embl.de/users/anders/HTSeq/doc/count.html</a>	
DESeq2	<a href="http://genomebiology.com/2014/15/12/550">http://genomebiology.com/2014/15/12/550</a>	v1.40.1
R analysis software	<a href="https://www.r-project.org/">https://www.r-project.org/</a>	
Ingenuity Pathway Analysis software (IPA)	Qiagen	
DAVID Bioinformatics Resources 6.8	<a href="https://david.ncifcrf.gov/">https://david.ncifcrf.gov/</a>	v6.8
Gene Set Enrichment Analysis (GSEA)	<a href="https://www.gsea-msigdb.org/gsea/index.jsp">https://www.gsea-msigdb.org/gsea/index.jsp</a>	v0.11.0
STRING	<a href="https://string-db.org/">https://string-db.org/</a>	v10.5
Nephroseq database	<a href="https://www.nephroseq.org/">https://www.nephroseq.org/</a>	v4
<b>Other</b>		
RNeasy® Mini kit for total RNA isolation	Qiagen	74104
No. 140 mesh sieve, 106 $\mu$ m opening	Fisher Scientific	04-881-10Z
No. 80 mesh sieve, 180 $\mu$ m opening	Fisher Scientific	04-881-10W
No. 200 mesh sieve, 75 $\mu$ m opening	Fisher Scientific	04-881-10BB
TruSeq Standard total RNA with Ribo-Zero Globin Complete kit	Illumina	20020612

### RESOURCE AVAILABILITY

#### Lead contact

Further information and requests for resources and reagents should be directed to and will be fulfilled by the lead contact, William E. Smoyer ([William.Smoyer@nationwidechildrens.org](mailto:William.Smoyer@nationwidechildrens.org))

#### Materials availability

This study did not generate new unique reagents.

### Data and code availability

All RNA sequencing data have been deposited at GEO and are publicly available as of the date of publication. Accession number is listed in the [key resources table](#).

This paper does not report original code.

Any additional information required to reanalyze the data reported in this paper is available from the [lead contact](#) upon request.

## EXPERIMENTAL MODEL AND STUDY PARTICIPANT DETAILS

All procedures were approved by The Abigail Wexner Research Institute at Nationwide Children's Hospital Institutional Animal Care and Use Committee (IACUC protocol AR13-00005) and performed in accordance with the National Institutes of Health Guide for the care and use of laboratory animals. For *in vivo* animal studies, male Wistar outbred rats were purchased from Envigo. Rats were of 5–6 weeks of age, approximately 125–150 g at delivery. Rats were housed in ventilated cages housed with 4 rats per cage with *ad libitum* irradiated chow and *ad libitum* water and acclimated to the NCH facility for 1 week prior to starting experiments. Rats are provided a hiding device, crinkle paper, and a Nylabone for enrichment and observed daily. The room is maintained at  $72 \pm 2^\circ\text{F}$  and 30–70% humidity and kept on a 12h/12h light/dark cycle with automatic light timers, all parameters are monitored and logged daily. Sentinel animals are maintained in the room for disease detection with dirty bedding from each cage being placed in the sentinel cage.

Spot urines were collected on day 0, prior to injection, for baseline proteinuria measurement. Rats were randomly assigned for A) control or disease and B) vehicle or drug treatment with at least one animal per treatment group in each cohort. Nephrotic syndrome was induced in rats with a single intravenous tail vein injection of puromycin aminonucleoside (PAN; P7130, Millipore Sigma) prepared in sterile saline at 50 mg/kg with 500  $\mu\text{l}$  being injected and control rats receiving 500  $\mu\text{l}$  saline injection. Healthy and disease control rats groups ( $n = 4/\text{group}$ ) received vehicle oral gavage vehicle solution (0.5% methylcellulose, 0.025% Tween-20), while the treatment received: (i) GC (Methylprednisolone; 15 mg/kg; Solu-Medrol, Pfizer Inc., New York, NY) by intraperitoneal (IP) injection daily or (ii) Pioglitazone (Pio; 10 mg/kg; Enzo; Farmingdale, NY) by oral gavage starting directly after PAN/saline injection. Pioglitazone was prepared in the vehicle solution noted. Rats were monitored and weighed daily, and spot urines were collected on day 11 for proteinuria measurement. Rats were sacrificed and kidneys were harvested, decapsulated, and washed with ice cold PBS for glomerular isolation.

## METHOD DETAILS

### Proteinuria measurement

UPCR was measured by Antech Diagnostics (Morrisville, NC) using standard techniques that are fully compliant with Good Laboratory Practice regulations, as we have previously published (22).

### Glomerular isolation

Glomeruli were isolated by standard sequential sieving method.<sup>60,61</sup> Briefly, kidney cortex was pared using curved scissors into a Petri dish with cold PBS, minced well, drained, and washed onto pre-moistened No. 80 sieves. Using a squeeze bottle, minced kidneys were then washed thoroughly and transferred to a No. 140 sieve that was stacked on a No. 200 sieve. Kidney material was then gently pressed through the No. 140 sieve using the bottom of a cold 250 ml beaker, and the isolated glomeruli collected on the No. 200 sieve. Glomeruli were then washed with cold PBS to remove contaminants, collected into labeled 50 ml conical tubes, spun at  $\sim 1500$  rpm for 3 min, and the glomerular precipitate suspended in RLT buffer (Qiagen, Germantown, MD) containing 0.1% v/v  $\beta$ -mercaptoethanol (M6250 Sigma, St. Louis, MO). Glomeruli were homogenized through a 21-gauge needle then processed for total RNA isolation.

### Total RNA isolation and DNA digestion for RNA-Seq samples

Total RNA from the isolated glomeruli was extracted using the RNeasy Mini Kit (74104, Qiagen, Germantown, MD) according to the manufacturer's instructions. The purity and yield of RNA was determined by measuring the absorbance at 230, 260 and 280 nm. Briefly, 1  $\mu\text{g}$  of RNA was subjected to DNase (AM2222; Ambion, Thermo Fisher Scientific, Waltham, MA) digestion at  $37^\circ\text{C}$  for 30 min followed by DNase inactivation with 5 mM EDTA at  $75^\circ\text{C}$  for 10 min.

### RNA Library preparation and sequencing

RNA quality was assessed using the Agilent 2100 Bioanalyzer and RNA Nano Chip Kit (Agilent Technologies, Santa Clara, CA) to ensure that the RNA Integrity Number (RIN) was  $\geq 7$ . RNA-seq libraries were then generated using TruSeq Standard total RNA with Ribo-Zero Globin Complete kit (Illumina, San Diego, CA). Briefly, ribosomal RNA (rRNA) was removed from 350 ng of total RNA with biotinylated, target-specific oligos combined with Ribo-Zero rRNA removal beads from the Human/Mouse/Rat Globin kit. To generate directional signals in RNA seq data, libraries were constructed from first strand cDNA using TruSeq Standard total RNA with Ribo-Zero Globin Complete kit (Epicentre Biotechnologies, Madison, WI). Briefly, 50 ng of rRNA-depleted RNA was fragmented and reverse transcribed using random primers containing a 5' tagging sequence, followed by 3' end tagging with a terminal-tagging oligo to yield di-tagged, single-stranded cDNA. Following purification using a magnetic bead-based approach, the di-tagged cDNA was amplified by limit-cycle PCR using primer pairs that anneal to tagging sequences and add adaptor sequences required for sequencing cluster generation. Amplified RNA-seq libraries were purified using AMPure

XP System (Beckman Coulter, Brea, CA). The quality of libraries was determined via Agilent 2200 TapeStation using High Sensitivity D1000 tape and quantified using Kappa SYBR®Fast qPCR kit (KAPA Biosystems, Inc, Wilmington, MA). Approximately, 90–125 million paired-end 150 bp reads were generated per sample using the Illumina HiSeq4000 platform. Raw data were converted to FASTQ using Illumina's bcl2fastq application. Sequencing adapters matching at least 6 bases were then removed from the reads, as well as low-quality bases (<10) using v1.10 of cutadapt (<https://cutadapt.readthedocs.io/en/stable/index.html>). An alignment report was also generated, using custom scripts, and manually reviewed to ensure that at least ~80% of reads aligned to the expected reference, and that at least ~50% of the reads aligned to features annotated as protein coding.

### RNA-seq data analysis

Each sample was aligned to the Rnor\_6.0 assembly of the *Rattus norvegicus* reference from the National Center for Biotechnology Information (NCBI) using version 2.5.0c of the RNA-Seq aligner STAR (<http://bioinformatics.oxfordjournals.org/content/29/1/15>). Transcript features were identified from the general feature format (GFF) file that came with the assembly from the NCBI. Feature coverage counts were calculated using HTSeq (<http://www-huber.embl.de/users/anders/HTSeq/doc/count.html>). The raw RNA-Seq gene expression data were normalized, and post-alignment statistical analyses and figure generation were performed using DESeq2 (<http://genomebiology.com/2014/15/12/550>) and custom analysis scripts written in R. Comparisons of gene expression and associated statistical analyses were made between different conditions of interest using the normalized read counts. All fold-change values were expressed as test condition/control condition, where values < 1 were denoted as the negative of its inverse (note that there will be no fold change values between -1 and 1, and that the fold changes of "1" and "-1" represent the same value). Transcripts were considered significantly differentially expressed using a 10% false discovery rate (DESeq2 adjusted p value <0.1). Genes were removed from comparisons if they were not expressed above a threshold (0.5 reads per million) for most samples within each group. Criteria for the selection: (1) DEGs were filtered based on FDR <0.05 in PAN vs. Control, (2) FDR >0.05 in PAN + MP vs. Control, and (3) At least 3 columns per gene showed normalized counts (NC) > 25. Z-scores derived from normalized counts were used for heatmap construction, and centroid linkage hierarchical clustering was employed for heatmap analysis.

### Functional gene annotation tools

Functional gene analysis was performed by Ingenuity Pathway Analysis software (IPA), DAVID Bioinformatics Resources 6.8, NIAID/NIH, STRING functional protein association networks, and Gene Set Enrichment Analysis (GSEA). We utilized IPA for building drug-target interaction networks by exploring the connections between nuclear receptors, their agonists and the streamlined genes data using the IPA knowledgebase as the reference. We also used IPA's disease view and toxicity feature to link experimental data to understand biological functional and pharmacological responses.

The DAVID functional annotation tool aids in identifying biological processes associated with a gene list using gene co-occurrence probability. DAVID 6.8 contains information on >1.5 million genes from >65,000 species. The STRING database includes both known and predicted protein-protein interactions. These interactions stem from computational prediction, from knowledge transfer between organisms, and from interactions aggregated from other (primary) databases. The STRING database currently covers 24,584,628 proteins and 5,090 organisms. The GSEA was performed by the Bioconductor R package -cluster profiler (<https://bioconductor.org/packages/release/bioc/html/clusterProfiler.html>) using the Molecular Signatures Database (MSigDB) C2 curated gene set and Canonical Pathways (CP) as subcategory. GSEA identifies biological pathways that are enriched in a gene list more than would be expected by chance. GSEA progressively examines genes from the top to the bottom of a ranked list, increasing the enrichment score (ES) if a gene is part of the pathway and decreasing the score otherwise. The ES score is calculated as the maximum value of the running sum, and normalized relative to the pathway size, resulting in a normalized enrichment score (NES) that reflects the enrichment of the pathway in the list. Positive and negative NES values represent enrichment at the top and bottom of the list, respectively. C2 curated gene-sets collection in molecular signatures database (MSigDb) was used for GSEA.

### Publicly available human dataset validation

Nephroseq database (<https://www.nephroseq.org/>) was used to query gene expression in the Hodgkin MCD and FSGS dataset<sup>31</sup> generated from laser capture microdissection of 8–35 glomeruli from kidney biopsies and analysis with the Affymetrix X3P Array. Patients included had biopsy-proven MCD (n = 7) or primary classic FSGS (n = 8). Control kidney samples (n = 9) were taken from biopsies for minimal isolated proteinuria or hematuria (n = 7) or tissue from uninvolved portions of a kidney at the time of nephrectomy for tumor (n = 2) (NephroSeq: Hodgkin FSGS Glom). Also, the Mariani et al. 2022 glomerular dataset<sup>33</sup> was also used for analysis of gene expression (NephroSeq: Mariani Nephrotic Syndrome Glom). The study included 220 NEPTUNE,<sup>62</sup> 35 H3Africa,<sup>63</sup> and 30 ERCB<sup>64,65</sup> participants with biopsy-proven MCD or FSGS and compartment-enriched genome-wide kidney mRNA expression profiles. NEPTUNE (NCT01209000) is a prospective study of children and adults with proteinuria, recruited at the time of their first clinically indicated kidney biopsy.<sup>62,66</sup> ERCB is a European study of adults with biopsy tissue for gene expression profiling and cross-sectional clinical information.<sup>64,65</sup> H3 Africa is a prospective study of participants aged 15 years and above, eligible for a kidney biopsy, recruited in Nigeria and Ghana with estimated glomerular filtration rate (eGFR)  $\geq 15$  mL/min/1.73m<sup>2</sup> and proteinuria (albuminuria >500 mg/day).<sup>63</sup> For all cohorts, informed consent was obtained from individual patients or parents/guardians, on approval by Institutional Review Boards or local ethics committees of participating institutions. In NEPTUNE and H3 Africa, RNAseq was performed on manually micro-dissected kidney biopsy tissue that separated tubulointerstitial and glomerular compartments. In ERCB,

compartment specific transcriptomic profiles of the research core were generated using the Affymetrix microarray platform (Santa Clara, CA). The Woroniecka<sup>32</sup> dataset was also manually microdissected for glomerular and tubular compartments, with 5 glomeruli used for RNA extraction and analysis by Affymetrix U133 A2.0 expression arrays (NephroSeq: Woroniecka Diabetes Glom). Kidney samples were obtained from living allograft donors and surgical nephrectomies and leftover portions of diagnostic kidney biopsies to include n = 9 diabetic kidney disease (diabetic nephropathy, DN) and n = 13 control samples. Upregulation and downregulation of genes were summarized into a table format with p-values denoted as \*p < 0.05 vs. normal/healthy kidneys. Output from queries is presented in [Figures S2–S5](#) showing heatmaps of log2 median-centered intensity with Fold Change relative to normal kidneys/healthy living donor and associated p values.

### **In silico cellular deconvolution of rat glomerular RNAseq with mouse single cell RNAseq**

Deconvolution was based on a published comprehensive online atlas of gene expression in mouse glomerular cells.<sup>35</sup> This published paper did set a stage for the dissection of glomerular function at the single-cell level. The listed genes in the published paper for each cell type in the glomerulus were used as reference for our rat transcriptomics data where we subdivided our glomerular transcriptomes into cell-specific subgroups. To do so, we used a cut-off of  $\geq 500$  normalized mRNA counts (since the normalized mRNA counts varied from 0 to  $\sim 400,000$ ) to qualify that gene to be enriched in that cell-type specificity analysis. After applying this criterion, we identified 66 podocyte-, 43 mesangial-, and 42 endothelial-cell-specific genes. The normalized counts were converted to Z score to generate a heatmap illustrating each of these three cell-types specific gene clusters, including comparisons of mRNA changes among the Control vs. PAN vs. PAN + MP vs. PAN + Pio treatment groups.

### **QUANTIFICATION AND STATISTICAL ANALYSIS**

Statistical significance was determined by the unpaired Student's t test for single comparisons and one-way ANOVA (analysis of variance) or two-way ANOVA for multiple group comparisons, using the GraphPad Prism software version 8.00. p-values are indicated in the respective figures and figure legends. Data is represented as Mean  $\pm$  SEM. In all cases, p < 0.05 was considered statistically significant. N's (number of rats) and p-values for comparisons can be found in figure legends.